Progress in Polymer Science 37 (2012) 1051–1078

Contents lists available at SciVerse ScienceDirect

Progress in Polymer Science

journal homepage: www.elsevier.com/locate/ppolysci

Synthesis, properties and biomedical applications of poly(glycerol sebacate) (PGS): A review

Ranjana Rai*, Marwa Tallawi, Alexandra Grigore, Aldo R. Boccaccini*

Institute of Biomaterials, Department of Materials Science and Engineering, University of Erlangen-Nuremberg, 91058 Erlangen, Germany

ARTICLE INFO

Article history:
Received 11 August 2011
Received in revised form 24 January 2012
Accepted 27 January 2012
Available online 4 February 2012

Keywords:
Poly(glycerol sebacate)
Bioresorbable polymers
Biocompatible
Tissue engineering
PGS processing

ABSTRACT

Poly(glycerol sebacate) (PGS) is a biodegradable polymer increasingly used in a variety of biomedical applications. This polyester is prepared by polycondensation of glycerol and sebacic acid. PGS exhibits biocompatibility and biodegradability, both highly relevant properties in biomedical applications. PGS also involves cost effective production with the possibility of up scaling to industrial production. In addition, the mechanical properties and degradation kinetics of PGS can be tailored to match the requirements of intended applications by controlling curing time, curing temperature, reactants concentration and the degree of acrylation in acrylated PGS. Because of the flexible and elastomeric nature of PGS, its biomedical applications have mainly targeted soft tissue replacement and the engineering of soft tissues, such as cardiac muscle, blood, nerve, cartilage and retina. However, applications of PGS are being expanded to include drug delivery, tissue adhesive and hard tissue (*i.e.*, bone) regeneration. The design and fabrication of PGS based devices for applications that mimic native physiological conditions are also being pursued. Novel designs range from accordion-like honeycomb structures for cardiac patches, gecko-like surfaces for tissue adhesives to PGS (nano) fibers for extra cellular matrix (ECM) like constructs; new design avenues are being investigated to meet the ever growing demand for replacement tissues and organs. In less than a decade PGS has become a material of great scrutiny and interest by the biomedical research community. In this review we consolidate the valuable existing knowledge in the fields of synthesis, properties and biomedical applications of PGS and PGS-related biomaterials and devices.

Contents

* Corresponding authors. Tel.: +49 9131 85 20806; fax: +49 9131 85 28602.
E-mail addresses: ranjana.rai@ww.uni-erlangen.de (R. Rai), Aldo.Boccaccini@ww.uni-erlangen.de (A.R. Boccaccini).

0079-6700/$ – see front matter © 2012 Elsevier Ltd. All rights reserved.
doi:10.1016/j.progpolymsci.2012.02.001

1. Introduction

There is increasing need for sustainable medical therapeutics to treat ailments and diseases compromising the normal functions of the human body, or even for aesthetic purposes. This need will escalate as the human population continues to soar. To address the issue of sustainable medical treatment, the biomedical sector relies on research on biomedical materials involving the development of medical devices targeted for numerous applications beyond traditional implants and prostheses to include tissue engineering and control drug delivery vehicles. Tissue engineering has gained enormous interest as a means to restore, maintain and improve tissue function, particularly in the light of increasing demand for replacement tissues and organs. In this context, biomaterials play a pivotal role as the interaction between cells and biomaterials determine the success or failure of most tissue engineering approaches [1,2].

Among a range of available biomaterials, polymers represent materials of choice for numerous biomedical applications. Biocompatibility is a key property of biomedical polymers, *i.e.*, the ability of the material to perform with an appropriate host response without inflammation of the surrounding tissues [1]. The nature of any degradation products represents another important property of polymers for tissue engineering, *i.e.*, degradation products should be absorbed in the body and ultimately be removed *via* natural metabolic processes (*i.e.*, bioresorbability). Depending on their origin, polymeric biomaterials may be classified as either natural or synthetic. Owing to their origin natural polymers may positively enhance cell material interactions. However, this origin can potentially induce dangerous immune reactions [2]. On the other hand, with synthetic polymers, it is possible to produce biomaterials with wide-ranging and reproducible properties by tailored variations of the components and synthetic processes. Among the many synthetic and bioresorbable polymeric biomaterials suitable for biomedical applications, one such family currently attracting attention is poly(glycerol sebacate) (PGS). PGS is a chemically polymer, first reported in 2002 in the context of tissue engineering as a tough biodegradable polyester synthesized for soft tissue engineering [3]. PGS is relatively inexpensive, exhibits thermoset elastomeric properties [4], and is bioresorbable, *i.e.*, it can degrade and further resorb *in vivo*, with the degradation products eliminated through natural pathways as it is the case with other polymers [5,6]. In addition, PGS maybe tailored to achieve mechanical properties and degradation rates targeted to a particular application [3]. Owing to the positive attributes of PGS, within the span of a decade PGS has been explored for numerous biomedical applications, ranging from hard to soft tissue engineering, controlled drug delivery and tissue adhesives. As the research on PGS based medical applications is expected to continue, this review seeks to consolidate existing knowledge, encompassing synthesis technologies, material properties and key biomedical applications. Approaches for the modification of PGS and avenues for future research are also discussed.

2. Synthesis of PGS

The synthesis of PGS involves consideration of five criteria, dictated by the intended application [3]:

(1) The polymer must undergo hydrolytic degradation to minimize the variation in degradation kinetics caused by enzymatic degradation.
(2) Hydrolysable ester bonds should be incorporated in the structure.
(3) A low degree of cross-linking should be present in the polymeric chains.
(4) Crosslink chemical bonds need to be hydrolyzable and identical to those in the backbone to minimize the possibility of heterogeneous degradation.

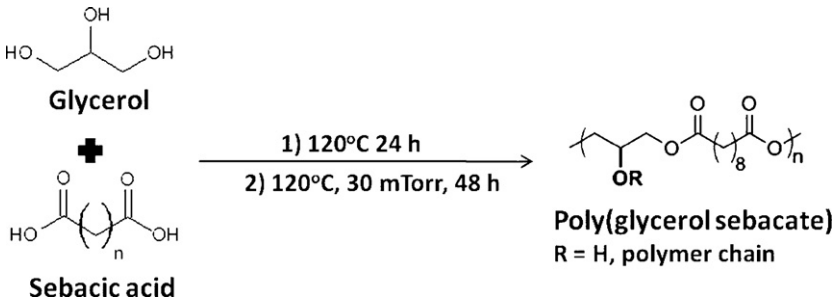

Fig. 1. Reaction scheme for the chemical synthesis of poly(glycerol sebacate). Adapted from [3].

(5) Starting materials have to be nontoxic, at least one should be trifunctional and at least one should provide hydroxyl groups for hydrogen bonding.

The common starting materials chosen for PGS synthesis are glycerol and sebacic acid. Glycerol ($CH_2(OH)CH(OH)CH_2OH$) is a basic building block for lipids which satisfies the design criteria mentioned above. Similarly, sebacic acid ($HOOC(CH_2)_8COOH$) is chosen as the acid monomer from the toxicological and polymer chemistry standpoints. Sebacic acid is the natural metabolic intermediate in ω-oxidation of medium- to long-chain fatty acids [3,7–10] and has been shown to be safe *in vivo* [3,11]. The US Food and Drug Administration (FDA) has approved glycerol to be used as humectant in foods, and polymers containing sebacic acid, *e.g.*, polifeprosan, have been approved for medical applications such as in drug delivery systems [3,4].

In the original investigation of Wang et al. [3] the polymer synthesis was carried out in two steps: (1) pre polycondensation step and (2) crosslinking. For the polycondensation process, equimolar mixtures (1 M) of glycerol and sebacic acid were reacted at 120 °C under argon for 24 h before the pressure was reduced from 1 Torr to 40 mTorr over 5 h. For the crosslinking step the prepolycondensed polymer (prepolymer) was further kept at 40 mTorr and 120 °C for 48 h. The reaction scheme of the final synthesis is shown in Fig. 1 [3].

This conventional method of a two-step synthesis *via* prepolycondensation and crosslinking has been mainly pursued for PGS synthesis. Although studies have been carried out to modify the properties of PGS by changing parameters such as the molar concentration of reactant mixtures [4] and synthesis temperature [12], the synthesis itself however, is normally carried out using the conventional method described above. This conventional method of PGS synthesis involves the use of rather harsh conditions, *e.g.*, temperature greater than 100 °C, and high vacuum. It is therefore not possible to polymerize the polymer *in vivo* and to introduce temperature sensitive molecules [13]. Nijst et al. [13] used a photopolymerization approach to address this limitation. The PGS prepolymer was chemically modified by introducing reactive acrylate moieties. This PGS with acrylate moieties, designated poly(glycerol sebacate) acrylate (PGSA), was cured using UV radiation in the presence of the photo-initiator 2-dimethoxy-2-phenylacetophenone (DMPA). Since crosslinking of vinyl bonds in PGSA can occur *via* both redox and photo-initiated free radical polymerization, Ifkovits et al. [14] investigated both redox and photo polymerization of PGSA. Using photopolymerization, the polymer could be cured rapidly within minutes at ambient temperature. This strategy drastically reduced the curing time to few minutes from the 48 h typically required using the conventional method. This approach also helped to overcome the limitation of thermally processing PGS, thereby increasing its processing and application possibilities By controlling the incorporation of acrylate moieties in the PGSA it was also possible to control the mechanical properties of the final acrylated PGSA [13,14].

3. Properties

Understanding the properties of any biomaterial in depth is the first step towards elucidating its potential for possible applications. PGS has been subjected to numerous studies to gain deeper understanding of its properties. The following sections cover these aspects of the development of PGS.

3.1. Physico-chemical properties of PGS

PGS is a transparent, almost colorless polyester. The chemical structure of PGS is given in Fig. 1 [3]. FTIR analysis carried out by Wang et al. [3] demonstrated that PGS exhibits peaks at 2930 cm^{-1} and 2855 cm^{-1} for alkane groups. An intense band at 1740 cm^{-1} occurs due to C=O stretching and at 1164 cm^{-1} due to C—O stretching; these are signature bands for ester linkages thus confirming that the polymer is a polyester [3]. The structural investigation of the PGS prepolymer has also been done using Nuclear Magnetic Resonance (NMR) spectroscopy [13]. Structurally, the hydroxyl groups attached to the carbon backbone contribute to the hydrophilicity of the polymer [3]. In fact, PGS has a water-in-air contact angle of 32° which is almost equal to the 31.9° contact angle value for flat 2.7 nm thick type I collagen films [3,15]. Carboxylic groups present in the sebacic acid are involved in the formation of the ester linkages during the crosslinking step. The crosslinking density increases as the curing time and curing temperature increase [16]. Jaafer et al. [17] reported that when the curing time increases, the FTIR spectrum of

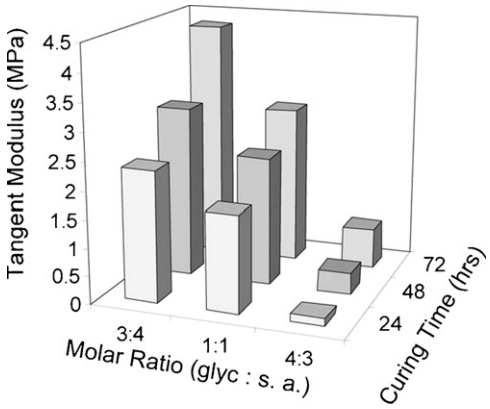

Fig. 2. Tangent modulus (at 10% strain) values for PGS cylinders with various processing parameters. Linear regression can be used to predict the modulus (70% power) from these two variables: modulus (MPa) = 3.607–1.410 × (ratio of glycerol:sebacic acid) þ 0.60 × (vacuum curing time in hours).
Data from [4]. (2010) Reproduced with permission of John Wiley and Sons.

PGS shows a reduction in the carboxylic acid O-H bend at 1418 cm^{-1}. In addition, FTIR results show the reduction in O—H stretch bands at 3300 cm^{-1}, signifying that acid groups further react with alcohol groups in the mixture to form ester bonds [17].

3.2. Mechanical properties

Tensile strength tests of PGS have shown that the material exhibits nonlinear stress–strain behavior, which is typical for soft elastomeric materials [3,16]. The typical stress strain curves of PGS are similar to that of vulcanized rubber. The elastomeric nature of the polymer is due to the covalently crosslinked, three-dimensional network of random coils with hydroxyl groups attached to its backbone; both the crosslinking and the hydrogen bonding interactions between the hydroxyl groups contribute to its elastomeric properties [3,18]. For example, PGS materials have average tensile Young's modulus in the range 0.0250–1.2 MPa, the ultimate tensile strength is >0.5 MPa and strain to failure greater than 330% [3,16,19]. The Young's modulus of PGS is between that of ligaments (kPa range) [20,21] and the myocardium of the human heart, which ranges between 0.02 and 0.5 MPa, and its maximum elongation is similar to that of arteries and veins, up to 260% [22].

The mechanical properties of PGS may be tailored by altering three processing parameters: (1) curing temperature, (2) molar ratio of glycerol to sebacic acid and (3) curing time [4,16,23]. In 2008, Chen et al. [16] demonstrated the influence of curing temperature on the mechanical properties of PGS, recording Young's modulus values of 0.056 MPa, 0.22 MPa and 1.2 MPa for curing temperatures of 110 °C, 120 °C and 130 °C, respectively. More recently, Kemppainen and Hollister [4] revealed the effect of altering the molar ratio of glycerol to sebacic acid and curing time on the mechanical properties of PGS. The results of the study are presented in Fig. 2 where an increase in the glycerol molar ratio is seen to decrease the tangent modulus and *vice versa.* In addition, the tangent modulus increases with increasing curing time.

The acrylate groups in PGSA facilitate an additional level of control [13]. This is because the number of acrylate moieties in PGSA dictates the concentration of cross-links in the resulting network, thereby influencing its mechanical properties [14]. The Young's modulus and ultimate tensile strength of photocured PGSA were linearly proportional to the degree of acryalation (DA). The Young's modulus of photocured PGSA varied between 0.05 MPa (DA = 0.17) and 1.38 MPa (DA = 0.54), and the ultimate strength between 0.05 and 0.50 MPa [13].

It has been also shown that PGS films exhibit stable mechanical properties, varying slightly when a cycling load was applied due to a stress softening process [24]. The stiffness of the film was shown to drop ~3% after the first two cycles, with an overall drop after 10 cycles of 5, 7, 9 and 14% for PGS containing 0, 5, 10 and 15 wt% Bioglass®, respectively [24]. Thus, PGS is a flexible elastomeric material, with the ability to undergo large reversible deformation with almost complete recovery in mechanically dynamic environments. This property makes PGS particularly attractive for soft tissue engineering applications. Also the flexible nature of the polymer makes it suitable for applications in difficult contours of the body, for which hard brittle polymers cannot be utilized.

3.3. Thermal properties

PGS is a partially semicrystalline polymer and therefore its thermal properties depend on the temperature relative to the glass to rubber transition temperature T_g of the amorphous phase and the melting temperature T_m of the crystalline phase. An early investigation on the thermal properties of PGS by Wang et al. [3] revealed two crystallization temperatures at −52.14 °C and −18.50 °C, and two melting temperatures at 5.23 °C and 37.62 °C. No glass transition temperature was observed above −80 °C, which was the lower detection limit of the instrument used in the study. DSC results indicate that the polymer is totally amorphous at 37 °C. Therefore, as with a vulcanized rubber, a PGS elastomer is a thermoset polymer [3]. In a study carried out by Cai and Liu [25] the PGS network exhibited a T_g at −37.02 °C and an additional broad melting transition at temperatures ranging from −20 °C to 40 °C. It also confirmed the observation made earlier by Wang et al. [3] that the polymer at 37 °C is totally amorphous. An important feature of the study of Cai and Liu [25] is the investigation of the shape memory behavior of PGS. The shape-memory effect was examined by a bending test as follows: a straight strip of the specimen was folded at room temperature, and then cooled to preserve the deformation. The deformed sample was then heated again at a fixed temperature, and the changes in shape with temperature were recorded (Fig. 3). The studies revealed that the three-dimensional network of PGS acted as the fixed phase and the amorphous phase acted as the reversible phase [25].

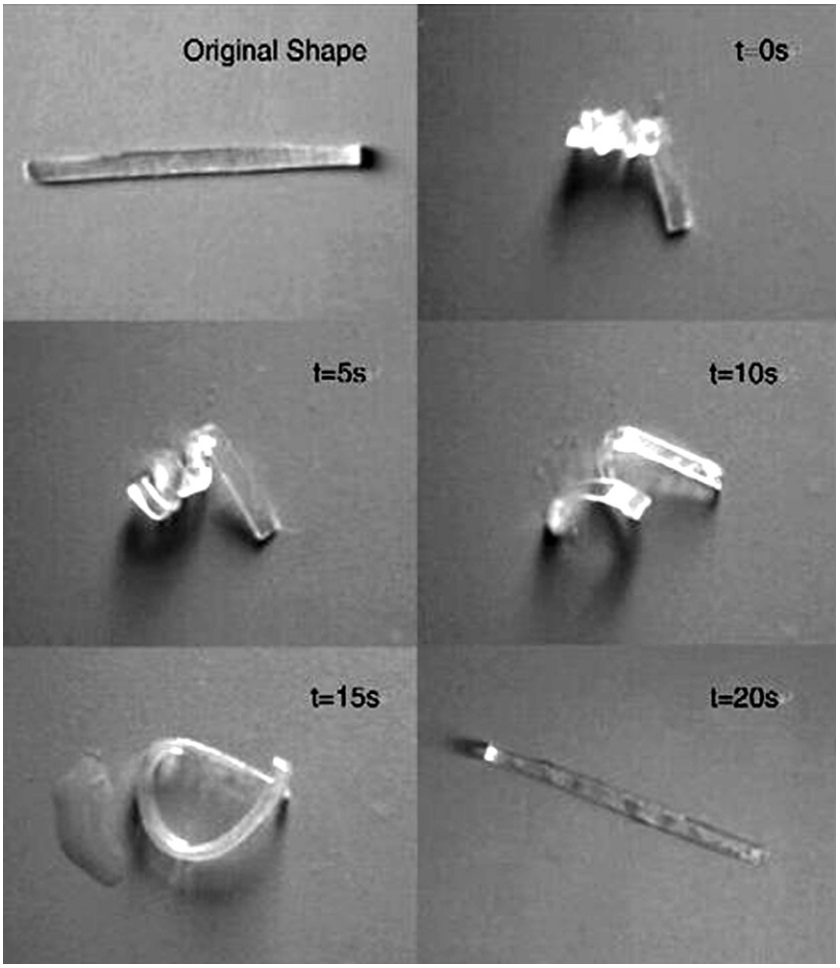

Fig. 3. Photographs showing the shape memory effect of PGS (recovery temperature 18 °C).
From Ref. [25]. (2008) Reproduced with permission of Elsevier.

3.4. Crystallinity and morphology

It is usually considered that the large and irregular pendant side groups present in polymers with long carbon backbone, inhibit close packing of the polymer chains in a regular three-dimensional fashion to form a crystalline array, thus resulting in their low crystallinity [26,27]. As mentioned above, thermal studies of PGS have revealed that it is a semi-crystalline polymer being, completely amorphous above 37 °C. Broad halos typical for amorphous polymers are observed in X-ray diffraction (XRD) studies on PGS [16]. Jaafer et al. [17] demonstrated that the degree of crystallization of PGS decreases significantly with increasing curing time and temperature, as revealed by DSC spectra. Fig. 4 shows the narrowing of the transition region, reduction in peaks magnitude and a general shift of the peaks towards lower temperatures as the curing temperature and time increase [17].

3.5. Degradation behavior

The degradation behavior of any material is an important characteristic, having profound impact on its applications, especially relevant for biomedical applications. Degradation is often a progressive event affecting the materials physiochemical properties over time. Combined with the mechanism of degradation, its kinetics and the possible toxicity of degradation products collectively affect the material's application potential. A number of studies have been carried out to understand the degradation of PGS both *in vitro* and under *in vivo* conditions [3,28]. It is now well established that PGS undergoes surface degradation; the main mechanism of degradation being cleavage of the ester linkages. Unlike bulk degradation mechanisms, for which the mechanical strength decreases well in advance of mass loss, thereby altering the geometry (shape and volume) of the polymer, in PGS, which undergoes surface degradation, slow loss of mechanical strength (tensile properties), relative to mass loss (per unit original area) occurs. As the mass loss changes linearly with time, detectable swelling and better retention of geometry are observed (Fig. 5) [3,17,29]. PGS degradation studies have demonstrated that it is difficult to correlate the *in vitro* the *in vivo* degradation behavior of PGS [3]. PGS exhibits an accelerated rate of degradation *in vivo* relative to that under *in vitro* conditions. For example, PGS

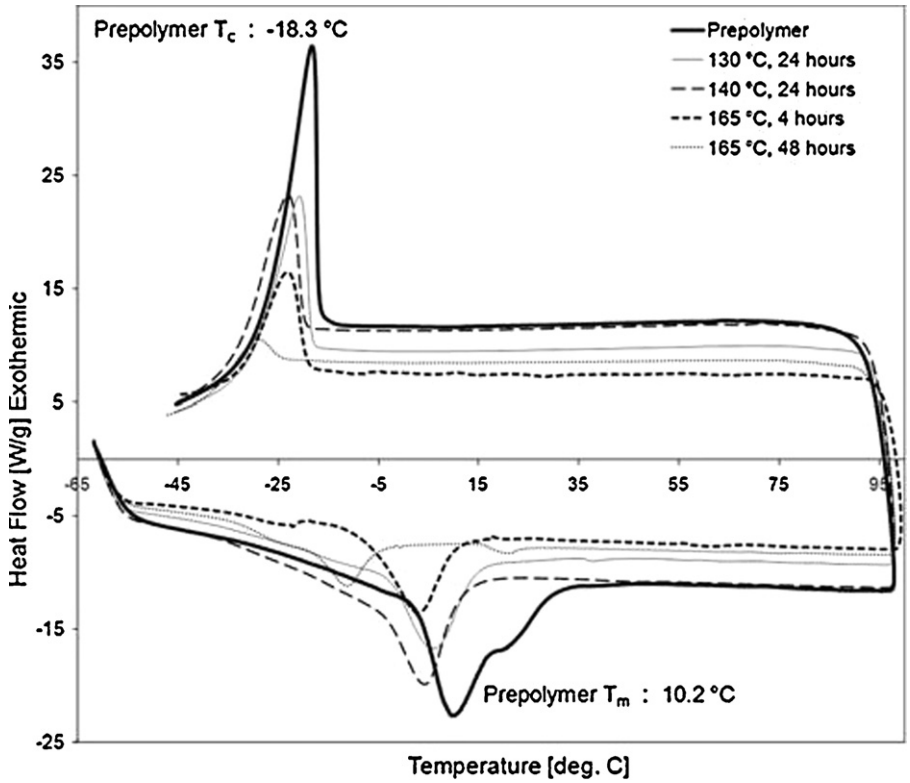

Fig. 4. DSC curves for PGS prepolymer and samples cured at different temperatures and durations. The recrystallization peak height at approximately −20 °C decreases with curing temperature and time. Although the curves signify the material is fully amorphous at room temperature, the recrystallization occurrence signifies that it is a semi-crystalline material. The slightly discernible steps between −30 and −40 °C signifies the materials glass transition temperature. This is observed to remain fairly constant for all the cure conditions.
From Ref. [17]. Reproduced with permission of Springer.

subcutaneously implanted in Sprague-Dawley rats was completely absorbed without granulation or formation of scar tissue [3]. Moreover the implantation site was restored to its normal histological architecture within 60 days [3]. On the other hand, under *in vitro* degradation condition at 37 °C in PBS the PGS film lost only 17.6% of its dry weight on day 60 [3]. Although it has been seen that the degradation rate of PGS *in vitro* cannot be correlated *in vivo* however, it may be noted that Liang et al. [30] found that the rate

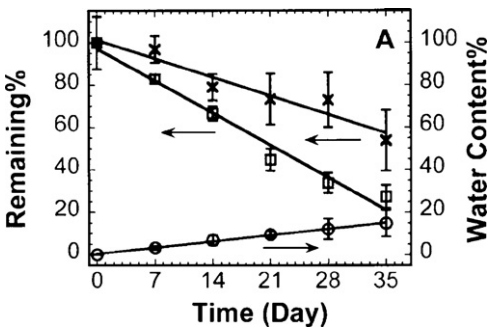

Fig. 5. *In vivo* degradation of PGS implants up to 35 days in young adult female Sprague-Dawley rats. Changes in mass (□); mechanical strength (×); water content (○). Steady almost linear changes of PGS implant properties upon degradation observed.
Data from [29]. Reproduced with permission of John Wiley and Sons.

of *in vitro* degradation of PGS sheets crosslinked at 125 °C for 2 or 7 days were 0.6–0.9 or 0.2–0.6 mm/month, respectively, in the culture medium, which is in the range of *in vivo* degradation rates (0.2–1.5 mm/month) of PGS.

The degradation kinetics of PGS can be controlled by varying processing parameters such as the curing time and temperature. Chen et al. [16] tailored the degradation of PGS to match the recovery kinetics of heart tissue. The degradation kinetics of PGS synthesized at 110 °C was faster than that of PGS synthesized at 120 °C, while PGS synthesized at 130 °C showed no evidence of degradation. These studies were carried out *in vitro* (in PBS and Knockout™ EMEM media).

3.6. Biocompatibility

The biocompatibility of PGS stems from the intrinsic biocompatibility of the starting reactants used in its synthesis. Gylcerol is the basic building block for lipids whereas sebacic acid is the natural metabolic intermediate in ω-oxidation of medium to long term fatty acids [3,9,11,12]. Hence the degradation products of PGS are often naturally metabolized in the body. Also, gylcerol and copolymers containing sebacic acid have been approved by the FDA for use in medical applications [3,8]. In addition, no catalysts or additives are used in the PGS synthesis process,

which avoids possible toxic effects in biomedical applications [31]. Last, as for any biomaterial, the biocompatibility of PGS is dependent on factors such as themorphology, surface porosity, density, surface hydrophilicity, surface energy and chemistry of the material, the environment where it is incorporated and the material degradation products [2,32,33].

Preliminary *in vitro* and *in vivo* biocompatibility test results have indicated that PGS is a suitable candidate material for several soft-tissue engineering applications [3,19,34–36]. Wang et al. [3] investigated the *in vitro* cell response to PGS coated glass Petri dishes seeded with NIH 3T3 fibroblast cells; as control PLGA coated dishes were used. PLGA was selected as the control since it is frequently used in tissue engineering applications and its resorption time matches that of PGS. Normal morphology and higher cell growth rate for PGS were observed compared to the PLGA sample, for which clusters formed and most of the attached cells adopted a long, thin, threadlike morphology, as tested by an MMT assay.

The *in vivo test* with Sprague-Dawley rats showed that the inflammatory response of PGS is similar to that of PLGA, but unlike PLGA, PGS induced little, if any, fibrous capsule formation [3]. Sundback et al. [19] investigated the inflammatory response of PGS and PLGA as assessed by the recruitment of lymphocytes, ED1 (marker for macrophages) and fibrotic tissue thickness. The lymphocytic and fibrotic reactions were mostly driven by the material degradation kinetics. As the PGS degradation behavior is based on surface erosion, the lymphocytic infiltrate level and the fibrotic zone thickness were seen to gradually decay throughout the implantation period. However PLGA was seen to undergo bulk degradation with significant swelling followed by rapid mass loss. This mass loss was shown to induce a tissue response spike; both the lymphocytic infiltration level and the fibrotic zone thickness increased significantly [19].

In tissue engineering, it is important that the cellular behavior affected by the degradation products of the biomaterial scaffold be considered for a comprehensive biocompatibility evaluation of the polymer used. To this end, assessment was also done on the cytotoxic effect of the degradation products of the polymers [19]. Schwann cells were exposed to PGS and PLGA extracts. The MTS tetrazolium cytotoxicity assay showed that Schwann cells cultured in both PGS and PLGA extracts had similar metabolic rates and they showed no cytotoxic effects in contact with the polymers [19].

A number of approaches are being used to increase the biocompatibility of biomaterials, such as surface treatment with NaOH, enzyme treatment, grafting of hydrophilic groups and coating of the polymeric surface with a biocompatible compound [37]. Therefore studies could also be carried out to translate these approaches to increase the biocompatibility of PGS. Studies on improving the biocompatibility of PGS have indeed been carried out and are mainly based on coating PGS surfaces with biocompatible molecules such as laminin, fibronectin, fibrin, collagen types I/III, or elastin [38]. As these molecules are natural components of the cellular environment, coating with such molecules will provide an additional impetus for improving the material–cell interactions and should expand the application potential of PGS.

4. Applications of PGS in medical applications

As described above, PGS is a remarkable polymer with attractive properties for biomedical applications primarily focused on soft tissue engineering applications such as cardiac muscle, vascular tissue engineering, cartilage, nerve conduits, retina, and tympanic membrane perforations. However, its medical applications are expanding further to include also targeted drug delivery and tissue adhesives. These applications are discussed in this section. The properties of PGS together with those of other biomaterials used in various medical applications included for comparison purposes are compiled in Table 1.

4.1. Tissue engineering applications

Tissue engineering is a multi-disciplinary field integrating cell biology, materials science, and surgical reconstruction, to provide living engineering constructs that restore, maintain, or improve tissue and organ function [51,52]. PGS is increasingly being used to develop scaffolds or matrices as cell delivery vehicles in a variety of tissue engineering approaches. The scaffold must be biocompatible, provide a conducive surface for the cells to adhere, must be able to guide and organize the cells in the required manner and must support cell growth, whereby cells should be maintained in a viable state by effective diffusion of nutrients and release of waste. Once new tissue is formed, the scaffold must degrade in a controlled manner and the degradation products must be non-toxic and well tolerated in the body [51]. Since many soft tissues in the body have elastomeric properties, successful tissue engineering usually requires the development of compliant (elastomeric) bioresorbable materials that can sustain and recover from prior deformations without adversely affecting the surrounding tissues; PGS is thus a material of choice in the context of soft tissue regeneration.

4.1.1. Cardiac tissue engineering

Cardiovascular diseases (CVDs) are the number one cause of death globally [53]. By 2030, almost 23.6 million people will die from CVDs, mainly from heart disease and stroke. These are projected to remain the single leading cause of death [53]. Myocardial infarction (or heart attack) is one of the major causes of death in patients suffering from CVD [53].

In post myocardial infarction, the heart undergoes a three-step healing process characterized by inflammatory, proliferative and maturation phases [54]. During this period, the matrix metalloproteases (MMPs) are activated, which degrades the extracellular matrix, resulting in myocyte slippage [55,56]. Progressive remodeling of the myocardium to a non-contractile fibrous scars tissue occurs, which leads to increased wall stress in the remaining viable myocardium. This process, results in a sequence of molecular, cellular, and physiological responses that lead to LV dilation and ultimately to the end stages of heart failure or congestive heart failure (CHF)

Table 1
Compilation of relevant properties of various polyester-based biomaterials (natural and synthetic) used in biomedical applications.[a]

Polymer	Origin	Polymer type (E or T)	Young's modulus	Tensile strength (MPa)	T_m (°C)	T_g (°C)	Degradation mechanism–hydrolysis	Degradation time	Application area	Reference
PGA	Synthetic	T	7–10 GPa	70	225	36	Surface	Faster degradation; 6 months *in vivo*	Hard and soft tissue engineering; drug delivery	[39,40]
PLGA fibers	Synthetic	T	40.4–134.5 MPa	2.1–2.6	159.75	59.25	Bulk	32% weight loss observed at 5 weeks *in vitro*	Hard and soft tissue engineering; drug delivery	[41,42]
PLLA or PDLLA	Synthetic	T	1–4 GPa	30–80	182.4	65.1	Surface	Slow degradation, at least 4 years *in vivo*	Hard and soft tissue engineering; drug delivery	[43–45]
PCL	Synthetic	T	343.9–364.3 MPa	10.5–16.1	59 to 64	−60	Surface	Slow degradation of up to 4 years in certain conditions *in vivo*	Drug delivery, hard tissue engineering. Composites of PGS for soft tissue engineering	[46–48]
Absolute homopolymer of P(3HO)	Natural	E	1–1.2 MPa	1.8	46.60	−35.55	Surface	No data available for *in vivo* degradation	Soft tissue engineering, wound dressing	[37]
P(3HB)	Natural	T	3.5 GPa	43	169	1.9	Surface	24–30 months *in vivo*	Bone tissue engineering, drug delivery and biomedical devices	[49,50]
PGS	Synthetic	E	0.04–1.2 MPa	0.20–0.5	−25.4	6	Surface	60 days *in vivo*	Soft tissue engineering, drug delivery, tissue adhesive	[3,16]

[a] T = thermoplastic; E = elastomeric; T_m = melting temperature; T_g = glass transition temperature; PCL = poly(ε-caprolactone); PGA = polyglycolic acid; PGS = poly(glycerol sebacate); P(3HO) = poly(3-hydroxyoctanoate); P(3HB) = poly(3-hydroxybutyrate); PLGA = poly(lactic-co-glycolic acid) orpoly(lactic-co-glycolic acid); PLLA = poly(L-lactide acid).

[56,57]. Current available treatments for CHF are heart transplantation and the use of ventricular assist devices (VADs). However, these treatments are besieged with acute problems of donor heart scarcity and high VAD cost. In this context, cardiac tissue engineering approaches are increasingly of interest in the search for treatments for infarcted myocardium. Various aspects of cardiac tissue engineering may be found in the comprehensive reviews of Radisic and Novakovic [58], Chiu et al. [54] and Leor et al. [59].

PGS has attracted increasing attention as a suitable material for myocardial tissue engineering [16,28,33,60–63]. Most of the studies in this field have centered on the development of PGS based cardiac patches (Fig. 6) [16,28,33,60,61,64]. The aim of the tissue engineered cardiac patch is to deliver healthy cardiac cells onto the infarct region and provide left ventricular restrain *i.e.* mechanical support to the left ventricle,

For the successful development of a cardiac patch, it is important to match the mechanical properties of the matrix or scaffold material with that of the native myocardium. As mentioned above, Chen et al. [16] studied the effect of temperature control in PGS synthesis as an approach to produce PGS with varying stiffness. The study demonstrated that the stiffness of PGS films synthesized at temperatures in the range 110–130 °C varied from several tens kPa to ~1 MPa, which covers the range of the passive stiffness of the heart muscle. Although PGS films were non porous [16], many studies have also been carried out on porous PGS scaffolds to tailor the mechanical properties matching that of the native heart [65]. Matching the stiffness of the PGS substrate to that of the cardiac muscle becomes particularly important as the substrate stiffness can have an effect on the phenotype of heart cells and on their functional properties [66].

Native myocardium is composed of cardiomyocytes, cardiac fibroblasts (CFs) and endothelial cells [54]. Cardiomyocytes are aligned in parallel to the heart wall and are the most physically energetic cells in the body, contracting more than 3 billion times in an average human lifespan and pumping over 7000 L of blood per day along 100, 0000 miles of blood vessels [58]. CFs contributes to the structural, biochemical, mechanical, and electrical properties of the myocardium. It also secretes regulatory and extracellular matrix (ECM) molecules, and couple gap junctions; all these have an effect on the cardiomyocytes behaviour [61,67–71]. The interaction between cardiomyocytes and CFs also affects the composition of the ECM. Studies have therefore also been carried out to understand the interaction of PGS with cardiomyocytes and CFs both *in vitro* and *in vivo* to assess if PGS films could be successfully integrated with such biological cues like cells and signaling molecules [28,61,64]. Furthermore, *in vitro* studies have provided valuable insights about the materials interaction *in vivo*. In this respect, an important study demonstrated that PGS films were able to support beating cardiomyocytes derived from hESC for up to 3 months without interruption. No significant difference was observed in the beating rates of the cardiomyocytes on the tissue culture plate, preconditioned PGS (immersed in DMEM medium for 6 days prior cell seeding) without any gelatin coating and gelatin coated PGS films [28]. This study, therefore demonstrated, that only preconditioned PGS surface without any gelatin coating, could provide desired attachment of the seeded cardiomyocytes, *i.e.* being able to retain healthy beating cells before implantation, to support the cells during surgical handling as well as to enable subsequent detachment of the cells from the surface [28].

It has been observed that CFs play an important role in the remodeling of engineered cardiac tissue [72]. Therefore pretreatment of PGS with fibroblasts has been carried out by Radisc et al. [61] to improve the properties of the engineered cardiac tissue by creating an environment to support cardiomyocytes attachment, differentiation and contractility. The study demonstrated that CFs could recover from the isolation procedure and remodel the polymeric scaffolds by depositing components of ECM and secrete soluble factors when seeded at low density during scaffold pre-treatment. Thus, the scaffold was conditioned to provide a native-like ventricular environment and support tissue assembly when the myocytes were added. *In vivo* studies using rat models have been carried out using acellular PGS constructs. When implanted a scaffold over the infarcted myocardium in a nude rat model, the scaffold remained in the ventricular wall after 2 weeks *in vitro*. It was also observed that the scaffold was vascularized (Fig. 7) [61].

Biomimetic approaches with PGS as a matrix have also been carried out to find solutions for myocardial tissue engineering (MTE) [33,64]. Cardiomyocytes have high oxygen demand, rely on unobstructed oxygen supply and are physiologically embedded in a delicate capillary network [73]. In a study carried out to mimic this scenario, scaffolds were fabricated to provide an *in vivo* like oxygen supply to the cells in PGS constructs consisting of a cell population of both myocytes and nonmyocytes (fibroblasts) [64]. To mimic the capillary network, a highly porous PGS scaffold fabricated using salt leaching technique was used in which parallel arrays of channels of $377 \pm 52\ \mu m$ in diameter were introduced [64]. To mimic the role of hemoglobin, the channel array was perfused with a culture medium at a flow velocity of ~500 μm/s (comparable to that of blood flow in native heart), supplemented with a synthetic oxygen carrier (oxygen^{TM}, perfluorocarbon emulsion). Constructs perfused with unsupplemented culture medium served as controls. The results showed that the constructs cultivated in the presence of perfluorocarbon (PFC) contained higher amounts of DNA, cardiac markers (troponin I, connexion-43) and exhibited significantly better contractile properties, as compared to the control constructs. Electron microscopy revealed that cells were present on both the channel surfaces and within the constructs of both groups [64].

The shear stress resulting from the circulating blood flow can have an effect on cells, hence in native myocardium the CMs are shielded from direct contact with blood by endothelial cells [63]. Low values of shear stress due to the circulating blood flow may induce phenotypic changes in cardiac cells, including elongation. However, higher values of shear stresses (*e.g.*, $\geq 2.4\ dyn\ cm^{-2}$) [63,74] have been shown to have detrimental effects on cardiac cells, inducing cell death and apoptosis [63]. When exposed to excessive shear stress, CMs were seen to round–up and

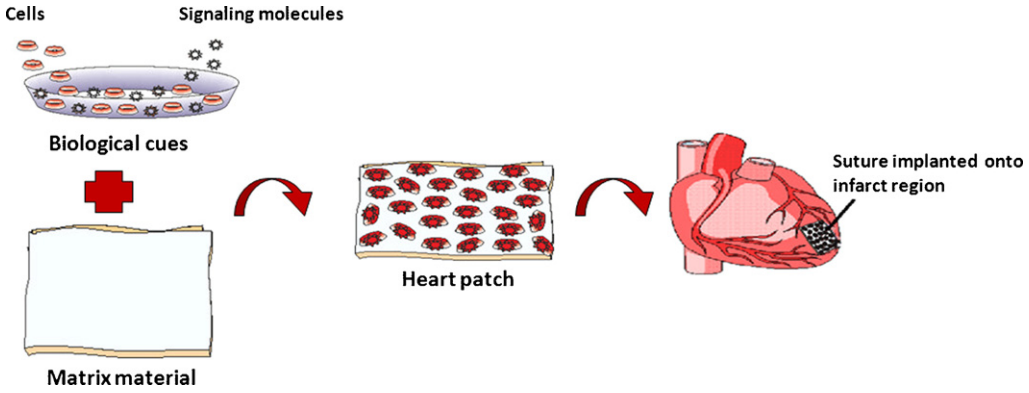

Fig. 6. Tissue engineering approach for the development of PGS (matrix material) based cardiac patch. Adapted from [56].

show signs of dedifferentiation [62,63,70,71]. Therefore, in another investigation by the same group [63] studies were carried out to find the optimal flow rate in perfusion to control oxygen supply and shear stress. A mathematical model was developed to determine the optimal channel spacing in the PGS scaffold, and the flow rate that would result in optimal oxygen concentration in the entire tissue space. This model was not only useful for studies involving channeled PGS scaffolds perfused with a PFC emulsion supplemented by a culture medium, but could also be extended to scaffolds perfused with pure culture medium [63].

Cardiac muscle fibers are highly branched and hierarchically surrounded and embedded in a 3D collagen network comprising distinct endomysial [75], perimysial [76] and epimysial levels of organization that resemble a honeycomb network [77]. This collagen architecture maintains the spatial registration of heart cells to enable cardiomyocyte contraction during systole while also protecting the cells from over-extension during diastole, thereby contributing to the robust, elastomeric material properties required for cardiac pump function [76,77]. This complex structure imparts cardiac anisotropy, *i.e.*,

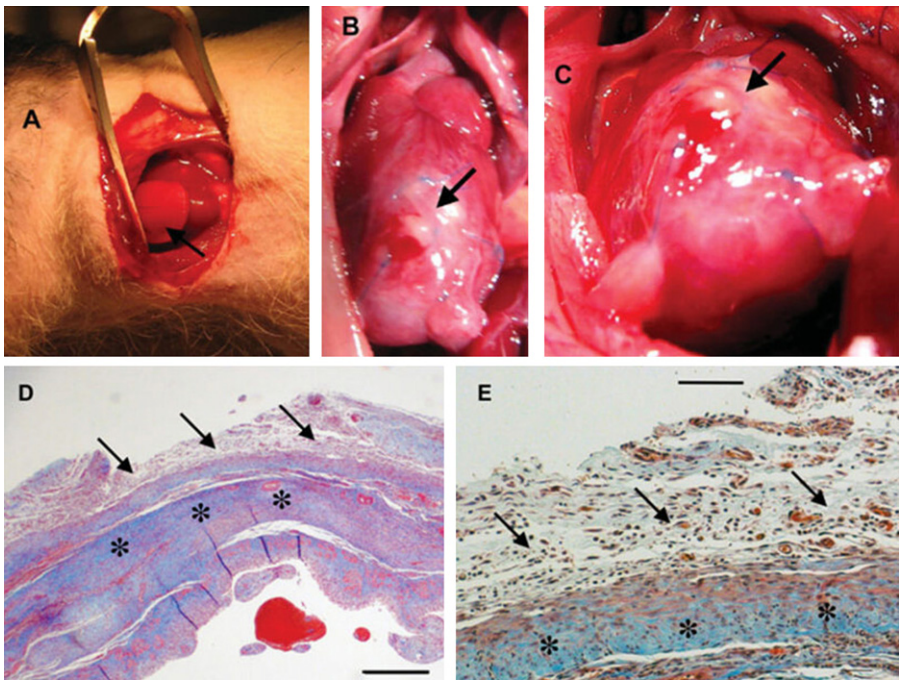

Fig. 7. Interactions between PGS scaffold and *in vivo* environment: implantation in a rat heart infarction model. According to results of Radisc et al. [61] (A) Implantation of the elastomer scaffold in a nude rat after induction of myocardial infarction by occlusion of the left anterior descending coronary artery. The scaffold (1 cm diameter × 1.5-mm thick disc) was sutured over the entire infarct bed (arrow). (B and C) Macroscopic view of the area at 2 weeks following implantation. (D) Cross-sectional view of the graft–host interface at 2 weeks (Mason's trichrome staining, collagen stains blue). Note excellent integration between the graft (arrows) and host (stars). (E) Higher magnification view of image D. Note the formation of multiple blood vessels within the graft, which were connected to the native circulation as evidenced by the presence of intraluminal red blood cells. Scale bars: 0.5 mm (D), 100 μm (E).
From Ref. [61] Reproduced with permission of John Wiley and Sons.

direction-dependent electrical and mechanical properties [33,73,77]. Accordingly, PGS scaffolds have been fabricated with accordion-like honeycomb (ALH) structure to mimic the native human myocardium [33]. These constructs exhibit anisotropic properties to promote parallel heart cell alignment. The ALH scaffold was microfabricated using excimer laser microablation technique in which modification of PGS to integrate a preferred (anisotropic) plane of flexibility into the scaffold material was carried out [33]. The scaffold seeded with neonatal heart cells demonstrated preferential heart cell alignment within 2 week of culture. During this period the scaffold was also able to retain anisotropic mechanical properties and withstand *in vitro* fatigue loading mimicking the dynamic physiologic epicardial strains. Mechanical properties similar to those of native rat right ventricular myocardium were also achieved after optimization of the polymer curing time [33]. Recently, Jean and Engelmayr [60] carried out finite element (FE) simulations and a homogenization approach to predict the anisotropic effective stiffness of the ALH PGS scaffold. This study showed that the FE model could be useful in designing variations in the ALH pore geometry that would then simultaneously provide proper cardiac anisotropy and reduced stiffness to enhance heart cell mediated contractility [60]. In another study the ALH structure was further exploited in combination with an additional porous layer [65]. A multi-layered PGS scaffold with controlled pore microarchitecture was fabricated, combined with heart cells, and cultured with perfusion to engineer contractile cardiac muscle constructs. In this construct design, one-layered (1L) scaffolds with accordion-like honeycomb shaped pores and elastomeric mechanical properties were fabricated by laser microablation of PGS membranes. Then, two layered (2L) scaffolds with fully interconnected three dimensional pore networks were fabricated by oxygen plasma treatment of 1L scaffolds followed by stacking with off-set laminae to produce a tightly bonded composite. When seeded with cardiomyocytes isolated from 1 to 3 days old neonatal Sprague Dawley rats, the 3D pore microarchitecture allowed cells to be readily seeded throughout its full thickness [65]. The porosity also allowed mass transport to and from centrally located cells by interstitial perfusion. The 1L and 2L scaffolds were mechanically stable over 7 days of culture with the heart cells under static and perfusion conditions. The laser-microablated PGS scaffolds exhibited effective stiffness ranging from 220 to 290 kPa. The ultimate tensile strength and strain-to-failure were higher than those of normal adult rat left ventricular myocardium. When subjected to electrical field stimulation the 7-day constructs contracted in response to the signals. Excitation thresholds were unaffected by scaffold scale-up from 1L to 2L. The 2L constructs exhibited reduced apoptosis, increased expression of connexin-43 (Cx-43) and matrix metalloprotease-2 (MMP-2) genes, and increased Cx-43 and cardiac troponin-I proteins when cultured with perfusion as compared to static controls [65].

Electrospinning, a convenient processing method to fabricate scaffolds mimicking native cardiac extracellular organization, has also been investigated using PGS. Ravichandran et al. [78] prepared PGS/gelatin core shell fibers by electrospinning to develop cardiac patches. Gelatin fibers were also electrospun for comparison. When subjected to mechanical evaluation, the PGS/gelatin fibers showed a Young's modulus value of 6 MPa and elongation at break of 61%. The contact angle value for the fibers was 7°. Cell–material interaction was assessed by seeding the electrospun fibers seeded with a coculture of mesenchymal stem cells (MSCs) and cardiomyocytes. Cell-scaffold interactions analyzed by cell proliferation, analysis of the expression marker proteins like actinin, troponin-T and platelet endothelial cell adhesion and cell morphology all revealed that the fabricated scaffolds possessed good biocompatibility, demonstrating the potential of spun PGS/gelatin core shell fibers with dual population of MSCs and cardiomyocytes for cardiac patch applications [78].

As the dynamic *in vivo* and *in vitro* environment differ, it is critical to assess the performance of any scaffold material *in vivo*, which ideally must be monitored serially and noninvasively [79]. Pertaining to this, Stuckey et al. [79] used magnetic resonance imaging to evaluate the *in vivo* performance of three patches made of PGS, poly(ethyleneterephathalate)/dimer fatty acid (PED) and TiO_2 reinforced PED (PED–TiO_2) grafted onto infarcted rat hearts. Patch free rat infarcted heart was used as a control. The results showed rapid *in vivo* degradation of PGS in comparison with its degradation *in vitro*. However, the PGS patch mechanically compatible with the rat heart was found to be successful in reducing hypertrophy, giving it potential for limiting excessive postinfarct remodeling [79].

4.1.2. Vascular tissue engineering

A number of studies have been carried out investigating the application of PGS for vascular tissue engineering. These investigation included the development of tubular based PGS constructs for engineering of blood vessels [80,81], the study of material cell interactions [35,82], the evaluation of the physiologic compliance of PGS based arterial constructs [34] and its hemocompatibility assessment [83]. Tubular PGS scaffolds were first created by Gao et al. [80], using an outer Teflon model with an inner sacrificial mandrel composed of paraffin wax. During scaffold preparation this inner space was filled with salt particles of 75–150 μm. The salt was fused at 37 °C and 88% relative humidity for 8 h following which the resultant salt template was dried. PGS dissolved in tetrahydrofuran (THF) was then introduced into this salt template. After the evaporation of the solvent the mandrel and the paraffin were removed. The PGS was cured and the salt particles leached out. The resultant tubular structure obtained had an internal diameter of 5 mm, wall thickness of 1 mm and a length 60 mm. The scaffold was approximately 95% porous with interconnected pores (75–150 μm) and a large fraction of micropores (5–20 μm) [80]. The fabrication of PGS tubular structures was further improved by another study of Crapo et al. [81]. In this study tubular scaffolds were prepared using three different types of mandrels. Scaffold type I used a paraffin mandrel, scaffold type II used a rigid polytetrafluoroethylene (PTFE) mandrel and scaffold type III used a heat shrinkable (HS) mandrel. The heat shrinkable mandrel sleeve, made of food-grade acrylatedpoly(olefin) (outer diameter (OD) 5.28 mm, and inner diameter (ID) 4.76 mm)

[4], was placed around a stainless steel rod encased by PTFE tubing to further reduce scaffold defects by reducing salt template disruption and adhesion to the mandrels. The scaffold fabrication process using the type III molds and HS mandrels was similar to the other fabrication processes, with two additional steps. After drying the salt template the poly(olefin) sleeve was removed by shrinking it onto a metal rod at120 °C (<5 min) and cooling the salt template to 20 °C before obtaining the final scaffold. Scaffolds fabricated with the heat-shrinkable mandrel had higher yield, fewer defects, more homogeneous wall thickness and microstructure, and higher porosity. These interconnected micropores should facilitate good cell-to-cell interaction and mass transport. When seeded with smooth muscle cells in a bioreactor, the optimized scaffold retained 74% of cells, which proliferated and formed a confluent cellular layer after 21 days of *in vitro* culture [81].

Endothelial cells (ECs) and smooth muscle cells (SMCs) play a pivotal role in vascular tissue engineering. ECs form a nonthrombogenic lining in the lumen of the vessel and SMCs form the vasoresponsive medial layer that bears the majority of the circumferential load. The interactions between ECs and SMCs are critical for the proper function of blood vessels. Endothelial progenitor cells (EPCs) play a critical role in blood vessel formation, differentiating into ECs, and most likely SMCs as well. The interaction of baboon endothelial progenitor cells (BaEPCs) and baboon smooth muscle cells (BaSMCs) cultured on PGS films and PGS constructs has been also investigated [35]. Cytocompatibility studies showed that PGS scaffolds and films provided a compatible surface for attachment and proliferation. Histological evaluations indicated that the BaSMCs were distributed throughout the scaffolds and synthesized extracellular matrix. In fact the biocompatibility of the seeded cells on PGS was similar to that observed on the tissue culture plate control. Typical normal cobblestone morphology by BaEPCs and spindle shaped by BaSMCs were observed under phase contrast microscopy. Immuofluorescent staining revealed that von Willebrand factor and a-smooth muscle actin were expressed by BaEPCs and BaSMCs, respectively [35].

Compliance mismatch is a significant challenge to long-term patency (the condition of being open) in small-diameter bypass grafts because it causes intimal hyperplasia and ultimately graft occlusion [34]. Recently, Crapo and Wang [34] engineered small arteries using elastomeric polymers PGS and PLGA under dynamic mechanical stimulation to produce strong and compliant arterial constructs. The final polymer constructs had thickness of $282 \pm 18\,\mu m$ for PGS and $290 \pm 17\,\mu m$ for PLGA, respectively. Similarly, porosity was $84.6 \pm 0.6\%$ for PGS scaffolds and $84.2 \pm 0.9\%$ for PLGA scaffolds. The luminal surfaces of PGS and PLGA scaffolds appeared similar. *In vitro* cell culture studies were carried out in a pulsatile perfusion bioreactor using adult baboon arterial smooth muscle cells (SMCs) cultured under cyclic strain for 10 days. Porcine carotid arteries were used as a positive control. After 10 days the seeded SMCs were found to co-express collagen and elastin giving rise to engineered arterial constructs with physiologic compliance. Scaffolds were significantly stronger after culture regardless of the material, but the elastic modulus of PLGA constructs was an order of magnitude greater than that of PGS constructs and the positive control. Also, arteries and PGS scaffolds exhibited elastic deformation and recovery whereas PLGA showed plastic (permanent) deformation. The compliance of arteries and PGS constructs was equivalent at the pressures tested. It was also found that altering the scaffold material (from PLGA to PGS) significantly decreased collagen content and significantly increased insoluble elastin content in constructs without affecting soluble elastin concentration in the culture medium. PLGA constructs contained no appreciable insoluble elastin [34]. One major contributing factor in the compliance mismatch observed for engineering vascular constructs is the challenge encountered with the synthesis of mature elastin [82]. Elastin provides elasticity and compliance to native arteries. It has been seen that arterial elastic fibers that are arranged into circumferentially organized elastic lamellae, allows arteries to maintain their original configurations from variations in hemodynamic stress [82,84]. However, synthesizing mature elastin has been a real challenge. Lee et al. [82] reported for the first time the preparation of mature and organized elastin in arterial constructs made up of porous PGS construct without any aid of exogenous factors or viral transduction. Smooth muscle cells of both baboon and porcine origins were used to develop the arterial constructs using porous PGS scaffold cultured in a pulsatile flow bioreactor. Three types of scaffolds with large (75–90 μm), medium (45–53 μm), and small (25–32 μm) pores were studied. Compared with larger pores, small pores increased SMC alignment, elastin and collagen production, burst pressure, and compliance. Circumferentially organized extracellular matrix proteins including elastin and multilayered SMCs expressing calponin and α-smooth muscle actin were revealed by histological analysis. Biochemical analysis demonstrated that the constructs contained mature elastin equivalent to 19% of the native arteries. Mechanical tests indicated that the constructs could withstand up to 200 mmHg burst pressure and exhibited compliance comparable to native arteries. These results show that nontransfected cells in PGS scaffolds in unsupplemented medium produced a substantial amount of mature elastin within 3 weeks, and the elastic fibers had similar orientation to that in native arteries (Fig. 8) [82].

Biomaterials intended for long-term contact with blood must not induce thrombosis, antigenic responses, destruction of blood components, and plasma proteins [85]. Motlagh et al. [83] investigated these aspects of hemocompatibility of PGS. PGS biphasic scaffolds were prepared by dip-coating glass rods with PGS acetone solution and then recoating the scaffolds with porous poly(1,8-octanediol citrate) (POC). Biphasic scaffolds consist of an outer porous phase and an inner non-porous phase. The thrombogenicity (platelet adhesion and aggregation) and inflammatory potential (IL-1b and TNFa expression) of PGS were evaluated using fresh human blood and a human cell line (THP-1). The activation of the clotting system was assessed *via* measurement of tissue factor expression on THP-1 cells, plasma recalcification times, and whole blood clotting times. Glass, tissue culture plastic (TCP), poly(L-lactide-co-glycolide) (PLGA), and expanded polytetrafluorethylene

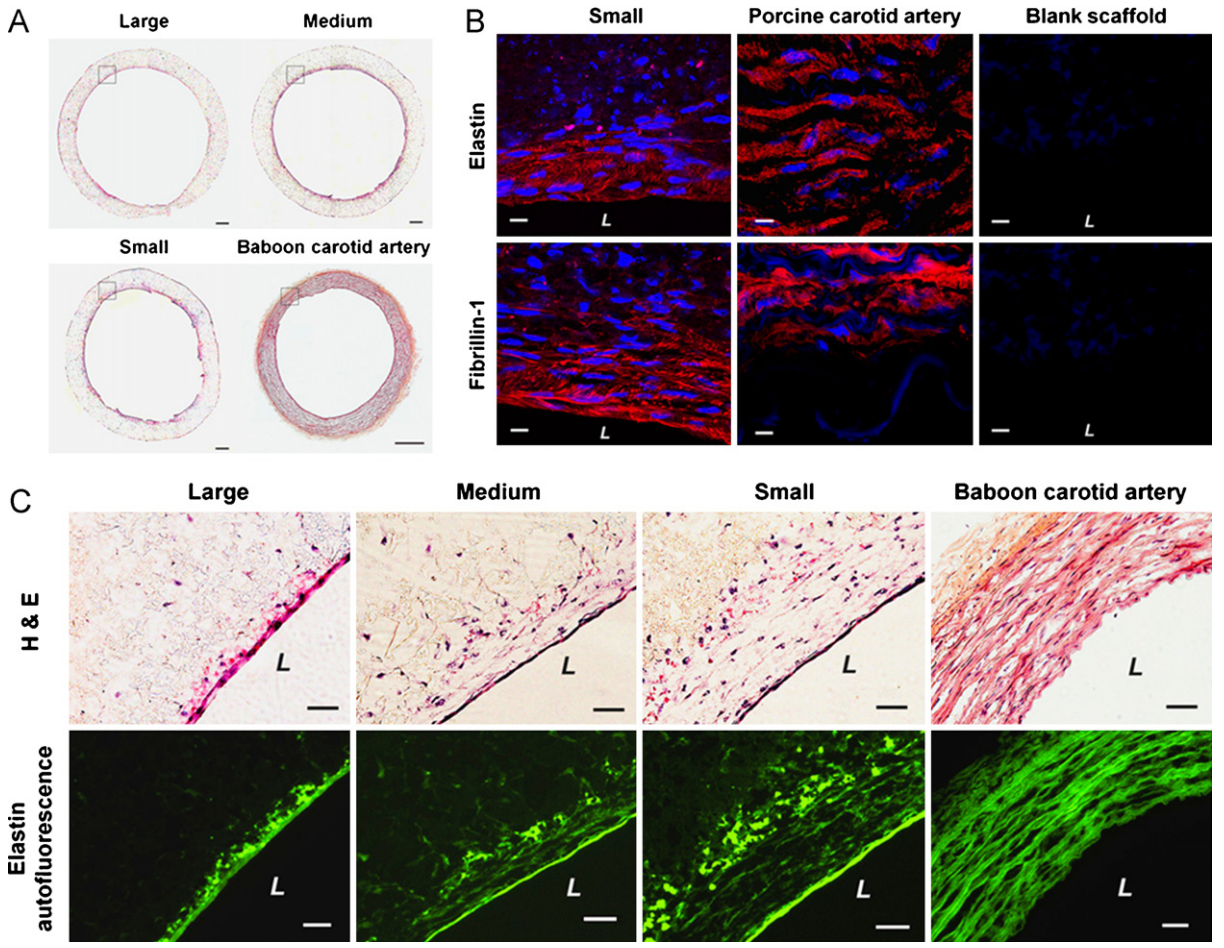

Fig. 8. ECM proteins and elastic fibers in PGS constructs and native arteries according to Lee et al. [82]. (A) H&E staining of the complete cross-section. (B) Immunofluorescence staining of elastin and fibrillin-1. Nuclei stained blue by Hoechst dye. Porcine carotid artery was used as a positive control. Blank scaffold showed no positive staining. Negative control with secondary antibody alone was also performed, but omitted to save space. L: lumen. (C) Partial magnification of the box shown in A and corresponding elastin autofluorescence. Magnification: 4× for A, 60× for B, and 20× for C; scale bar: 500 μm for A, 10 μm for B, and 50 μm for C.
From Ref. [82]. Reproduced with permission of National Academy of Sciences, United States.

(ePTFE) were used as reference materials. Relative to platelet attachment on glass (100%), attachment levels on ePTFE, PLGA and PGS were 61%, 100%, and 28%, respectively. PGS elicited a significantly lower release of IL-1b and TNFa from THP-1 cells than ePTFE and PLGA. Similarly the THP-1 cells showed decrease expression when exposed to PGS, in comparison to other reference materials. Plasma recalcification and whole blood clotting profiles of PGS were comparable to or better than those of the reference polymers tested [83]. This study suggested that PGS is a suitable hemocompatible material, however further studies are needed to characterize the hemocompatibility *in vivo* [83].

All these studies therefore show a possible avenue for the use of PGS to engineer non-thrombogenic vascular grafts with physiologic compliance.

4.1.3. Cartilage tissue engineering

Articular cartilage is a complex living tissue that lines the bony surface of joints. It can withstand millions of cycles of loading, exhibiting little or no wear under normal conditions [86]. It therefore provides a reduced friction surface enabling the joints to bear very large compressive loads. This ability of articular cartilage is attributed to the complex structure and composition of its extracellular matrix which possesses mechanical properties that are anisotropic, nonlinear and viscoelastic [86]. Although articular cartilage enables joints to withstand cycles of high load bearing activities, depending on the extent and location of damage, articular cartilage cells can self-heal when injured. This is however not always the case as articular cartilage lacks vasculature, and therefore has little or no capacity to repair itself [4,87]. Hence, tissue engineering approaches have been gaining momentum to engineer new or replace damage cartilage. In this context several materials have been investigated for matrix support or as scaffold material. The first study on exploring PGS as a scaffold material for cartilage tissue engineering was carried out by Kemppainen and Hollister [4]. They fabricated 3D PGS scaffolds exhibiting designed

pore shapes, pore sizes, porosities and architecture using solid free-form fabrication methods. The scaffold possessed 48.1% ± 4.24 of porosity with pore diameters of 1.04 mm ± 0.04. Finite element analysis predicted the modulus value of the fabricated scaffold from the basic PGS bulk properties studied, to range from 0.03 to 1.13 MPa, *i.e.*, within the range of native articular cartilage. *In vitro* studies with seeded condrocytes on PGS scaffolds were carried out utilizing similar designed polycaprolactone (PCL) scaffold as positive control. The results showed higher expression of aggrecan (the main proteoglycan found in cartilage and a typical marker for differentiated chrondrocytes) on PGS scaffolds than in preseeded cells. Similarly the collagen 2 to collagen 1 ratio (called differentiation index) was higher on PGS scaffold when compared to the control PCL scaffold. These results indicate more chondrogenic gene expression on a PGS scaffold than on a PCL scaffold, therefore demonstrating the ability of PGS to produce a cartilaginous matrix [4]. Another study was carried out by the same group [87] on the material effects on cartilage regeneration for scaffolds with the same controlled architecture. 3D scaffolds of the same design were fabricated using each of the polymers PCL, PGS and poly (1,8 octanediol-co-citrate) (POC). Physical and *in vitro* cell culture studies (using porcine chondrocytes) revealed that although the scaffold architecture remained the same, the scaffolds fabricated from the three polymers showed differences in their physical properties and tissue regeneration in terms of cell phenotype, cellular proliferation and differentiation, and matrix production. After 4 weeks of *in vitro* cell work, POC showed the highest DNA, sulfated glycosaminoglycans (sGAG), differentiation index and the lowest hypertrophy and matrix degradation gene expression compared to PCL and PGS. Although PCL and PGS both promoted chondrocytes to proliferate and express genes related to cartilage formation, they were also found to promote gene expression for cartilage destruction and ossification. [87]. Since these studies gave contradictory results, additional research is essential to draw any conclusion on the suitability of PGS in cartilage regeneration approaches.

4.1.4. Retinal tissue engineering

The retina is an eye tissue that contains photoreceptor cells which transduct the light into electrical impulses used further by the neural network to create the visual information [88]. Retinal degenerative disease affects the photoreceptor functions and causes visual impairment. At the moment, no viable cure exists and attempts have been made in the area of retinal transplantation, which aims for a replacement of the diseased photoreceptors. A successful transplant would secure the survival of the graft photoreceptors without being rejected by the host. Furthermore, the photoreceptors should preserve the organization and structure that ensure the proper signal phototransduction to the host neurons [88].

Emerging transplantation methods include the insertion of an immature graft retina with well-organized photoreceptors [88,89] and targeted delivery of retinal progenitor cells (RPCs) in the subretinal space [36,90]. In both cases attempts have been made to identify the critical factors that could lead to a graft–host integration failure. The remaining inner retinal cells in the donor retina and the diseased host photoreceptors [89,91] hinder the formation of functional tissue and should therefore be removed prior to the graft implantation. When using RPCs the main challenges are the delivery, survival and differentiation of cells [90]. Solutions for these issues may involve polymeric, biodegradable membranes inserted in the subretinal space to either induce selective photoreceptor removal by temporary retinal detachment [89,91] or as a scaffold for RPCs support, delivery and differentiation [36,90]. The material used in retinal tissue engineering should have similar size and mechanical properties as the subretinal space, which implies high flexibility and extensive elongation, but it should be robust enough for surgical manipulation [92]. The membranes should also display non-cytotoxicity [36], no inflammatory and no immune response [92]. In addition the biomaterials suggested for this application should exhibit biodegradability through hydrolysis within 6 months [36] and adjustable properties by tailoring the composition [92]. In cell-seeded scaffolds, porosity is a fundamental requirement since it enhances cell attachment and survival [92], and pore microtopography could guide the differentiation of progenitor cells [36].

In this context, PGS membranes have been developed for three different purposes: to be placed in subretinal space alone [91], as a composite with a graft retina and surface modification [88,89] and as a scaffold for RPCs delivery [36,90]. When placed between the retinal pigment epithelium and the outer nuclear layer, PGS membranes act as a barrier in the blood flow from the choroids to the retina causing selective removal of the diseased host photoreceptors [91]. This is highly desirable since as a consequence the integration of a healthy photoreceptor layer would be enhanced. Composite grafts have been also created and transplanted in the subretinal space using PGS membranes and retinal tissue [88,89] (Fig. 9). In order to overcome the major challenge of graft–host integration, PGS membranes were modified chemically with peptides containing RDG sequence and physically with a layer of electrospun laminin and poly(epsilon-caprolactone) PCL nanofibers [89].

PGS scaffolds can also provide temporary structural support for RPCs, facilitating their differentiation and maturation. Replica molding [88–90] in combination with a cryo-sectioning technique [88,89] was used to produce thin membranes suitable for the subretinal space. The method involves a PDMS negative mold spincoated with a sucrose layer on its surface; PGS scaffold is cured in the mold and then removed. Membranes of 45 μm thickness with pores of 50 μm in diameter placed at a distance of 175 μm [36,90] were seeded with RPCs (Fig. 10). The pore diameter and pattern were established in accordance to cell nutritional requirements and could be changed in a reliable manner. Similar membranes (but non-porous) were created for blocking the flow of nutrients causing selective removal of the photoreceptor layer [91]. These membranes showed a complete degradation after 28 days *in vivo* [91]. A further step was the development of a composite graft containing a PGS membrane and immature porcine full-thickness retina to be transplanted in the same surgical step [89]. For

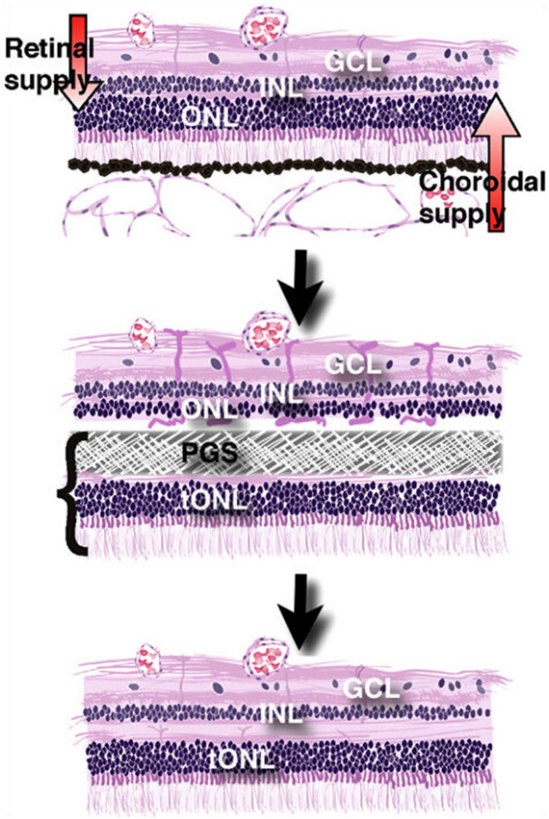

Fig. 9. Illustration of the composite retinal graft model. Top: The *in vivo* host retina is dependent on a dual blood supply. The choroid supplies the photoreceptors in the outer nuclear layer (ONL) while the retinal vessels supply the inner retinal cells in the inner nuclear and ganglion cell layer (INL and GCL). Middle: When the composite graft, consisting of photoreceptors in a transplant outer nuclear layer (tONL) fused with a PGS membrane, is placed in the subretinal space, the membrane blocks the nutritive support to the host ONL which induces ischemia and removes host photoreceptors. Bottom: Following PGS membrane degradation, the remaining inner retina of the host integrates with the transplanted photoreceptors (tONL) creating a new retina with all normal layers.
From Ref. [88]. Reproduced with permission of Elsevier.

an easier manipulation of the graft and reduced mechanical disruption of the retina, the membrane should be as flexible and therefore as thin as possible. Cryo-sectioning technique was employed for cutting PGS slices of 30 μm in thickness from a block of 3 mm produced by replica molding from a pre-polymer [89].

Young's modulus and the maximum strain at failure for the PGS porous scaffold were 1.66 ± 0.23 MPa and $113 \pm 22\%$, respectively [90], rendering an elastic and soft material similar to the retinal tissue with an elastic modulus of 0.1MPA and 83% strain at failure.

Cell adhesion [88,89] and morphologic adaptation [36] may be enhanced by chemical and topographical surface modifications. PGS scaffolds were coated with the extracelullar matrix protein laminin to promote cell attachment and differentiation of RPCs towards mature retinal phenotypes [36]. Short cell recognition peptides such as arginyl-glycyl-aspartic acid (RDG) were chemically coupled to the surface for better fusion between the PGS membrane and the retinal tissue sheet [88,89]. Coating PGS with electrospun nanofibers of laminin and poly (epsilon-caprolactone) resulted in improved attachment of porcine retinal layers, and can lead to graft–host neuronal connections [89]. The structure, geometry and degradation behavior of the nanofibers could influence axonal regeneration, cell adhesion and guidance [89].

Ex vivo and *in vivo* studies have shown that PGS membranes are well tolerated in the subretinal space. Further, PGS membranes facilitated the selective apoptosis of the host photoreceptors without provoking inflammation of the tissue [88,89,91]. Composite grafts with full-thickness retina survived in all transplants showing the lack of an immune rejection and formation of an outer nuclear layer of photoreceptors [88].

As previously mentioned, PGS scaffolds showed a high potential for the targeted delivery of progenitor cells to the retina and provided a suitable environment for their growth and differentiation into retinal neurons. Within 7 days of culture of murine RPCs on the scaffolds *in vitro*, cell infiltration and adhesion to pores was observed, followed by growth and partial differentiation [90]. In *ex vivo* experiments mRPC were integrated into retinal layers in normal and rhodopsin knockout retinal explant models [36]. PGS scaffolds seeded with mRPC were scrolled into a syringe and injected with minimal trauma *in vivo*, in the subretinal space of mice [36]. After one month it was seen that the cells migrated into the host retina and the protein expression patterns demonstrated that they differentiated into mature retinal neurons [36].

Although only limited amount of data are available, the results are encouraging for the application of PGS in retinal tissue engineering, based on PGS tailored properties. For this application, PGS mechanical properties are similar to retinal tissue and enable very thin membranes to be created and scrolled into a syringe. The surface biodegradation mechanism reduces the swelling, reduces the change of geometry and decreases the pH influence on the microenvironment. Finally, PGS shows a high compatibility with mRPC and promotes cell differentiation.

4.1.5. Nerve tissue engineering

Autologous autografts have been studied for bridging neural defects, however these materials may pose problems, such as donor site morbidity, scarcity of donor tissues and inadequate functional recovery [19,93]. Numerous natural and synthetic materials are being studied to overcome these problems for nerve tissue engineering. Artificial materials such as poly(glycolide) (PGA), poly(L-lactide) (PLLA), poly(DL-lactide-co-glycolide) (PLGA) [94–96], poly(lactide-ε-caprolactone) [97–99], biodegradable polyurethanes [100], poly(organo)phosphazenes [101], and trimethylene carbonate–caprolactone copolymers [102–104] proposed as neural conduits may exhibit unfavorable swelling and pro-inflammatory characteristics [19]. Owing to the favorable biocompatibility shown by PGS for other cell lines with respect to cardiac, vascular, cartilage and retinal tissue engineering [3,4,28], studying the biocompatibility of PGS for neural reconstruction applications has also been explored [19]. Several *in vitro* biocompatibility tests using primary Schwann cells and *in*

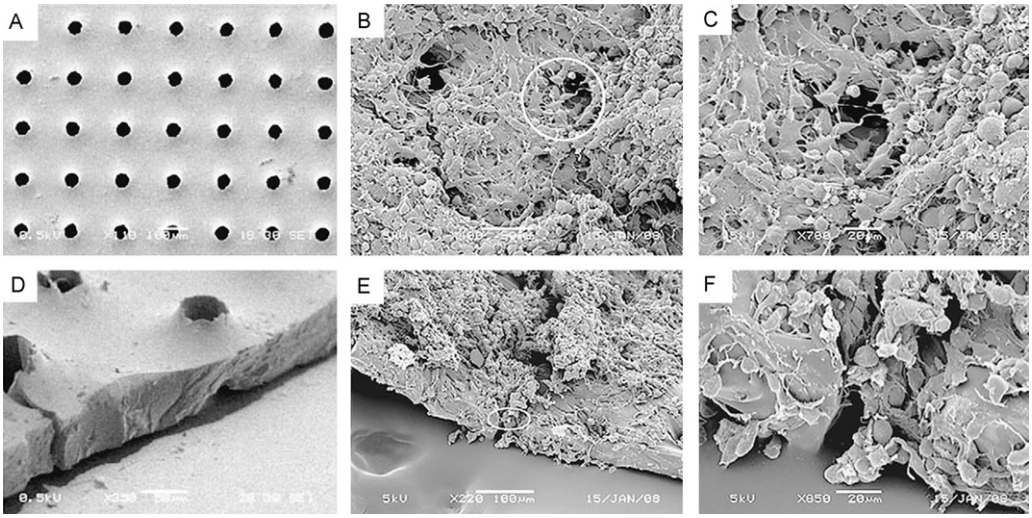

Fig. 10. SEM of PGS topology and mRPC adhesion. (A) Top view of a PGS scaffold of 45 mm in thickness with 50 mm diameter pores spaced 175 mm apart. (B) Top view of PGS seeded with mRPCs after 7 days of proliferation surrounding pore (circle). (C) Magnification of B showing individual mRPCs with flattened radial and bipolar morphology. (D) Side view of PGS scaffold showing the cone-like pore formation on the upper surface and 45 mm thickness. (E) Adhesion of neurospheres to the PGS surface, along the sidewalls, and within individual pores (circle). (F) Magnification of E showing spheroid mRPC infiltration into an individual pore.
From Ref. [36]. Reproduced with permission of Elsevier.

vivo acute and chronic tissue inflammation studies using male fisher rats were carried out. A PLGA material (50:50, carboxyl ended) possessing resorption time matching that of PGS was used as the control. *In vitro* studies *via* both direct and indirect contact tests experiments with Schwann cells revealed that PGS had no deleterious effect on the cells metabolic activity, attachment or proliferation, and did not induce apoptosis. The *in vitro* effects of PGS were similar or superior to those of PLGA. The *in vivo* tissue response to PGS was compared to the response to PLGA implanted juxtaposed to the sciatic nerve. The response was influenced by the degradation mechanism. *In vivo*, PGS demonstrated a favorable tissue response profile compared with PLGA, with significantly less inflammation and fibrosis and without detectable swelling during degradation. The lack of *in vitro* Schwann cell toxicity and minimal *in vivo* tissue response observed demonstrates that PGS can be a promising candidate material for neural reconstruction applications [19]. Application of PGS as a possible nerve conduit material is further enhanced by the fact that material properties such as Young's modulus, which ranges between several tens kPa to ~ 1 MPa, is close to the stiffness value of the *in situ* peripheral nerve (0.45 MPa) [19,105]. Also in comparison to other conduit materials such as lactide–glycolide and lactide–caprolactone copolymers, which undergo swelling of up to 100–300%, PGS undergoes degradation without much swelling. This behavior lowers the possibility of narrowing the tubular lumen by a swelled distorted matrix from, which can impede regeneration [19,106,107].

The results of the investigation by Sundback et al. [19] therefore, suggest that PGS possesses promising properties which could be exploited for application as nerve conduit materials. Nevertheless further studies need to be carried out to generate a large body of *in vitro* and *in vivo* data.

4.1.6. Repair of tympanic membrane perforations

Chronic tympanic membrane (TM) perforation often occurs as a sequel of tympanostomy tube placement and extrusion. With more than two million procedures performed annually, tympanostomy tube insertion is one of the most common surgical procedures [108,109]. Numerous techniques are available for the repair of chronic TM perforations, which are dependent on the size and location of the perforation and the status of the Eustachian tube function [109–111]. Transcanal myringoplasty techniques have been used for the treatment of centrally located small perforations (2–3 mm) using scaffolds made of rice paper, gel-film or fat to bridge the gap and facilitate epithelial migration and closure [109–111]. Wieland et al. [109] investigated for the first time PGS-engineered plugs to repair chronic tympanic membrane perforations in a chinchilla model. The PGS plug comprised four layers: bilayer central strut sandwiched between two flanges. The PGS plugs were inserted in stable 11 TM perforations. Gel-film overlay myringoplasty in 8 chinchillas was also studied for comparison. It was observed that of the 11 tympanic membranes implanted with PGS plug, 10 healed after weeks. Similarly for the gel-film, 6 of the 8 had healed at 6 weeks. Imaging of the medical mucosal and lateral epithelial surfaces of the tympanic membranes revealed PGS plug incorporation with neovascularization. Histology demonstrated a confluent cell layer on both sides of the graft and a decrease in the size of the plug owing to the surface erosion of the material. The results of this study suggested the feasibility of exploring further PGS as a scaffolding material for the repair of chronic TM perforations in humans. In addition, the tympanostomy tube shape of the PGS plug is also more structurally stable as opposed to currently used materials for myringoplasty such as gel-film, rice paper and fat [109].

4.2. Drug delivery

Controlled drug delivery is becoming increasingly applied because of the advantages that it offers over conventional delivery (drugs administered *via* an oral or intravenous route), including: controlled delivery of drugs locally at the target site, continuous maintenance of target drug concentration within the therapeutic window and reduced toxicity [112]. The integration of controlled drug delivery in tissue engineering applications for support and stimulation of tissue growth has further highlighted the importance of local drug delivery [113,114]. As in tissue engineering applications, the matrix or the scaffold used as a delivery vehicle plays a pivotal role in the success of the complete delivery system. This is because the matrix materials strongly influence the efficiency of drug encapsulation and its subsequent release kinetics. In addition, the matrix material used must be biocompatible and biodegradable.

Controlled drug delivery has also been applied for anti cancer therapy. This approach aims at delivering anticancer drugs to targeted cancerous tissues and to minimize systemic toxicity [115]. In this context, Sun et al. [115] investigated PGS as a bioresorbable drug delivery vehicle for anticancer therapy application. PGS implants were doped with the anticancer drug 5-fluorouracil (5-FU). Different weight % of doped 5-FU (2, 5, 7.5 and 10%) PGS samples were prepared and subjected to an in depth investigation involving chemical characterization, *in vitro* degradation, drug release behavior, *in vivo* degradation and tissue biocompatibility. *In vitro* degradation studies upto 30 days in PBS medium showed that all 5-FU-PGS samples retained their macroscopic geometry while undergoing degradation. Also, the *in vitro* degradation rate of 5-FU-PGS accelerated with increased concentration of the drug. Surface studies using scanning electron microscopy (SEM) showed that the surfaces of the degrading 5-FU-PGSs with higher concentration of 5-FU had irregular pits. These pit occurred due to the dissolution and diffusion of the 5-FU molecule in PBS, which facilitated increased water penetration and higher exposed surface area, leading to higher rate of polymer hydrolysis and degradation. This role of 5-FU in pit formation explained why irregular pits were observed in the degrading 5-FU-PGS samples with increasing drug concentration. The cumulative drug release profiles of 5-FU-PGSs exhibited a biphasic release with an initial burst release in the first day. Almost 100% cumulative release of 5-FU was found after 7 day for all 5-FU-PGSss. This release pattern was similar to that observed by the successful Gliadel® wafer commercially used for the treatment of recurrent glioblastoma and malignant gliomas. An *in vivo* investigation was carried out by inserting the 5-FU-PGS specimens intramuscularly on one side of the backbone of Wistar rats [115]. The 5-FU-PGS showed a much faster degradation rate *in vivo* than that *in vitro*. Histological studies using hematoxylin and eosin staining indicated no remarkable inflammation in the tissue surrounding 5-FU encapsulated PGS implants, suggesting that 5-FU-PGSs implants had good biocompatibility and no tissue toxicity. *In vitro* anti-tumor activity assay suggested that 5-FU-PGSs samples exhibited anti-tumor activity through sustained-release drug mode. These results therefore demonstrated successfully that PGS is a candidate for developing bioresorbable drug carriers for anticancer therapy. Similarly, studies carried out by Tobias et al. [116] were aimed at developing PGS based delivery devices that could be deployed into urological organs for the treatment of chronic prostatitis. The drug encapsulated in the study was ciprofloxacin-HCL (CIP), a fluoroquinolone antibiotic commonly used for the treatment of a range of infections. The device was developed by casting PGS into a tubular geometry with CIP packed into its core, with a micromachined release orifice drilled through its wall using a microablation method. The PGS drug delivery device functioned through a combination of osmosis and diffusion mechanisms to release CIP. These results demonstrated the efficiency of PGS in functioning as a semipermeable material for an elementary osmotic pump with controlled release of CIP [116]. All these studies therefore suggest that PGS can be successfully and efficiently used as matrix for encapsulating drugs. Such PGS drug delivery vehicles offer the added advantage that owing to the tailorable degradable nature of PGS, vehicles made of this polymer could be implanted at disease sites where device retrieval is restricted [116].

4.3. Other medical applications

Several other medical applications are suggested for PGS, two of which are reviewed in this section: use as a barrier material to prevent VP adhesions and as a surgical sealant. Postoperative adhesions occur in up to 94% of all patients who undergo abdominal procedures, frequently causing intestinal obstruction and requiring further operation [117–119]. It is reported that 84% of this postoperative adhesion is accounted by the adhesion that forms between the visceral and parietal peritoneum (VP adhesion) [119,120]. These adhesions result in small bowel obstruction (SBO) and present complications in further operations. Currently the effective approach to prevent these adhesions is the use of barriers placed between injured peritoneum areas to prevent apposition of injured surfaces [119,121,122]. One of the clinically relevant barriers used currently is Seprafilm (Genzyme, Cambridge, MA) [119,123–126] Seprafilm is a hyaluronic acid-based film with demonstrated anti-adhesive efficacy, however this film sticks to moist surfaces and cannot be repositioned once applied [126–129]. Consequently, up to 20% of this product is discarded during a typical abdominal operation owing to handling difficulties [119,129]. Therefore, owing to its superior mechanical properties, biocompatibility and resorbability PGS was evaluated for possible applications as a barrier material to prevent such VP adhesions [119]. The evaluation was performed in a rat peritoneal adhesion model. The animals were evaluated for the presence of VP adhesions at 3, 5, and 8 weeks. Moreover, the laparoscopic applicability of PGS films was demonstrated by placement into a juvenile porcine abdomen using standard laparoscopic equipment and techniques. A statistically significant 94% reduction in VP adhesion formation rate was observed between control animals (75%) and animals with a PGS film barrier (4.8%) [119]. PGS films were easily placed in the juvenile porcine abdomen and could be readily

repositioned without material loss or tissue damage, unlike Seprafilm. PGS barrier films were shown to be efficacious in reducing VP adhesions in the rat model. They were seen to be easier to handle and could be placed using standard laparoscopic techniques. These promising results suggest that PGS films will be effective barriers to adhesion formation for patients undergoing open and laparoscopic abdominal operations [119]. In another application, a surgical sealant was developed by polymerizing PGS and lactic acid [12]. The PGS-co-LA tissue sealant developed is liquid at 45 °C and solidifies into a soft wax like patch at body temperature. This difference in the physical state of the PGS-co-LA copolymer enables it to be used as a surgical sealant. The PGS-co-LA tissue sealant exhibited higher adhesive strength than either fibrin sealant or synthetic PleuraSeal™. In addition, the incorporation of lactic acid into the polymer PGS was seen to improve the cytocompatibility of the PGS-co-LA copolymer as opposed to pure PGS when assessed with SNL mouse fibroblasts [12].

4.4. Summary

Summarizing the previous sections it can be stated that PGS is widely gaining momentum for numerous medical applications. A number of relevant patents granted for medical devices are summarized in Table 2. In addition, other possible avenues for PGS applications in the medical sector could be as bioresorbable sutures and drug eluting stents. PGS can also be a promising polymer for developing bioresorbable pressure synthetic adhesives (PSA). Such PSA can find applications in wound coverings and closures, surgical drapes, electrocardiograph electrode mounts and transdermal drug delivery [37]. Considering applications of other flexible, bioresorbable polymers such as some polymers of the polyhydroxyalkanoate (PHA) family [37,130] similar range of applications are possible for PGS including, manufacture of medical surgical garments, upholstery, packaging, compostable bags, lids or tubs for thermoformed articles and making flushables that can degrade in septic tank systems like hygienic wipes and tampon applicators.

5. Processing technologies for PGS constructs

In tissue engineering and regenerative medicine, approaches involving contact guidance using oriented chemical cues and state of the art processing technologies have been implemented either individually or in conjunction, such as rapid prototyping, solid free form fabrication, micromolding, microablation and electrospinning to fabricate designed scaffolds with controlled architecture, including such features as surface topography (*e.g.*, parallel array of channels), porosity (well interconnected pores to achieve convective and diffusive oxygen transport) and mechanical properties similar to native tissues (*e.g.*, tailored structures to mimic anisotropic tissues) [33,64,131]. With these technologies, features of dimensions ranging from nano to microscale are now being introduced in advanced scaffold designs. In this context, investigations targeting several applications have been carried out to fabricate controlled structured scaffolds based on PGS. Fabrication of PGS is relatively uncomplicated since it may be either easily melted or solvent processed. The PGS prepolymer is soluble in a number of solvents such as 1,3-dioxolane, tetrahydrofuran, ethanol, isopropanol, and N,N-dimethylformamide [3]. Special designs of scaffolds based on PGS are discussed in this section.

5.1. Contact guidance

The presence of a three-dimensional surface topography resembling the structure of extracellular matrix proteins [132] and topographic features within the basement membrane containing submicron length scales [133] present important biophysical cues to cells [131]. Research is taking place to achieve contact guidance, *i.e.*, introduce topographical micropatterning at micro and nanoscales on PGS substrates to induce controlled cellular responses like desired orientation and morphology of cells [131]. Such oriented layer of cells in turn induces the self-assembly of additional consistently organized layers of cells and extracellular matrix [134]. Contact guidance has been observed in a variety of cell types, such as epithelial cells [135–137], fibroblasts [137–140] oligodendrocytes [141] and astrocytes [141]. One potential application of contact guidance is in the field of tissue engineering. Bettinger et al. [131] has conducted such studies on the microfabrication of PGS for contact guidance. Rounded features of sub-micron scale (down to 500 nm) have been introduced in PGS platforms by replica molding on sucrose coated microfabricated silicon. The final PGS substrates obtained by delaminating through sucrose dissolution in water had microstructures between 2 and 5 μm in wavelength and depth of 0.45 μm. When seeded with bovine aortic endothelial cells (bAECs) the PGS matrix was able to align the cells. SEM studies showed cells displaying preferential attachment of filopodia to the apex of the microstructures thus suggesting that cells have an inherent ability to detect local gradients in topography and to adhere preferentially. This work of Bettinger et al. [131] showed that round features on substrates can also promote cell alignment like that observed for sharp features.

In another study, the contact guidance of muscle cells (murine myoblast cell line C2Cl2) using PGS matrix was studied [134]. Micromolding and microablation were used to produce two distinct groups of PGS membranes (LINE and control, CTL) with and without struts, micropatterned with linear gratings and two distinct pore designs (square, SQ and rectangle, RECT). The fabricated PGS films had thickness of the order 250 μm and top to bottom pores of the order of 150–280 μm. The resulting scaffolds exhibited anisotropic elastomeric mechanical properties, an important requirement of muscle cells for their normal functioning (Fig. 11). The orientation of the cells along the axis was calculated using the angle of deviation (AD) of the cellular long axis with respect to the gratings and pore edge. The quantification was carried out based on SEM images. A progressive increase in cell orientation was observed, with SQ CTL < SQ LINE and RECT CTL < RECT LINE). These findings suggested that PGS scaffolds enabled cultured muscle cells to preferentially align in parallel to linear gratings and pore edges with significant individual and interactive effects of

Table 2
Summary of patents related to PGS and biomedical applications of PGS.

Patent	Title	Summary	Link
US 20110129436	Polyglycerolsebacate peritoneal adhesion barrier	The invention describes the use of PGS for preventing adhesions between two tissue surfaces.	http://patents.com/us-20110129436.html
US20040044403	Tissue-engineered vascular structures	The invention describes novel, less invasive and improved methods of tissue engineering of constructs that require an endothelial surface such as blood vessels and heart valves. The construct makes use of poly(glycolic-co-sebacic) and other sebacic acid derived copolymers.	http://www.freepatentsonline.com/y2004/0044403.html
US7722894	Biodegradable polymer	The patent claims the application of PGS for a number of medical and non-medical applications.	http://www.freepatentsonline.com/7722894.html
US20100168832	Scaffolds for artificial heart valves and vascular structures	The invention relates to scaffolds for artificial heart valves and vascular structures comprising a biocompatible block copolymer. Although materials are not described, sebacic acid polymer, as possible material is included.	http://www.freepatentsonline.com/y2010/0168832.html
US 4237317	Process for producing sebacic acid	The patent relates to the method for the preparation of sebacate.	http://www.freepatentsonline.com/4237317.html
US 20060085063	Nano- and micro-scale engineering of polymeric scaffolds for vascular tissue engineering	The claim describes a synthetic conduit made of PGS for vascular tissue engineering comprising, a substantially tubular body made of circumferential polymer fibers.	http://www.freepatentsonline.com/y2006/0085063.html
US 20090234332	Artificial microvascular device and methods for manufacturing and using the same.	The claim relates to the usage of PGS to develop artificial microvascular devices mimicking key features of physiological vascular networks. The device would enable better understanding of the efficacy of various chemical or biological compounds against diseases of the cardiovascular system.	http://www.freepatentsonline.com/y2009/0234332.html
W09942147	Biodegradable shape memory polymer	The claim relates to the synthesis, composition of biodegradable shape memory polymer; articles manufactured using it and their usage. Although the polymer is not described but it may involve PGS.	http://v3.espacenet.com/publicationDetails/biblio?CC=WO&NR=9942147&KC=&FT=E

surface topography and anisotropic pore design (Fig. 12) [134].

Research and development of fibers (nano to micron-size) have gained much prominence in recent years due to the heightened awareness of their potential applications in the biomedical field. Electrospinning is the most successful method for producing these fibers, and is a relatively simple process (general information about electrospinning is available in comprehensive reviews [142,143]). Fibrous scaffolds have attractive properties for tissue engineering as they mimic the structure of the extracellular matrix. Moreover the anisotropic nature of fiber aligned tissues, such as the meniscus of the knee, the annulus fibrosus of the intervertebral disc, and cardiac muscle can be engineered using electrospun fibers [144–146]. High surface area to volume ratio [147–149] and favorable handling of tensile loads while maintaining relatively low bending rigidities are attractive properties of fibrous scaffolds [149–151]. In addition electrospun fibers also provide contact guides for cell orientation and migration. Nano-/microscale surface topographies significantly influence cell behaviors such as adhesion, orientation, migration and proliferation by mimicking the topography of the ECM [149,152,153]. In this context a study has been carried out focusing on the manipulation of electrospun PGS scaffold architecture (*via* control of fiber alignment) and porosity (*via* inclusion of a sacrificial fiber population) to control cellular interactions *in vitro* as well as cellular population and matrix organization, *in vivo* [146]. In this work, Ifkovits et al. [146] studied the influence of PGS fiber alignment and scaffold architecture on contact guidance, *i.e.*, cellular interaction and matrix organization. Three scaffolds were fabricated using AcrPGS, by varying fiber alignment, *i.e.*, aligned fiber (AL), non-aligned (NA) and by introducing a PEO sacrificial polymer population (composite (CO)). PEO removal led to an increase in scaffold porosity and maintenance of scaffold anisotropy, as evident through visualization, mechanical testing, and mass loss studies. The ability of the scaffold architecture to influence cellular alignment was confirmed *in vitro* using neonatal cardiomyocytes. The alignment of the fibers and

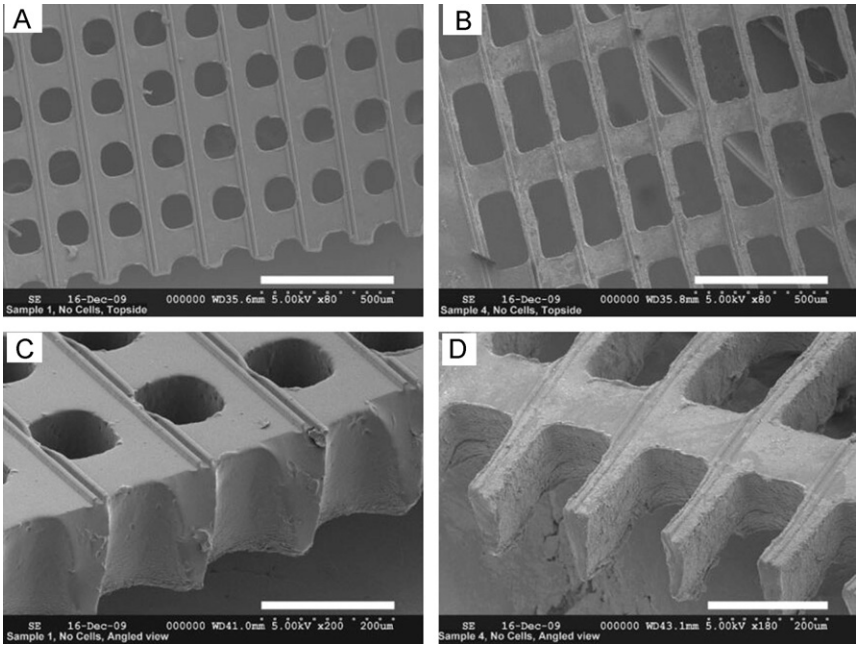

Fig. 11. Laser microablation of PGS: (A–D) SEMs at low and high magnification of membranes with micropatterning and (A and B) square pores or (C and D) anisotropic rectangular pores. Scale bars: (B and D) 500 μm, (C and E) 200 μm.
From Ref. [134]. Reproduced with permission of John Wiley and Sons.

cells was evaluated at 5 days post-seeding by determining the angle of intersection of a fiber or cell body with a horizontal reference line. As expected, a Gaussian distribution of fiber angles was observed for the AL and CO scaffolds, with the greatest quantity of fibers being oriented perpendicular to the reference line. However, this was not the case for the NA scaffolds where, as expected, the fibers displayed a random orientation. Similar trends in cellular alignment were also observed. The majority of cells seeded on the AL and CO scaffolds were oriented in perpendicular direction to the reference line, where the cells on the NA scaffold maintained a random orientation. When

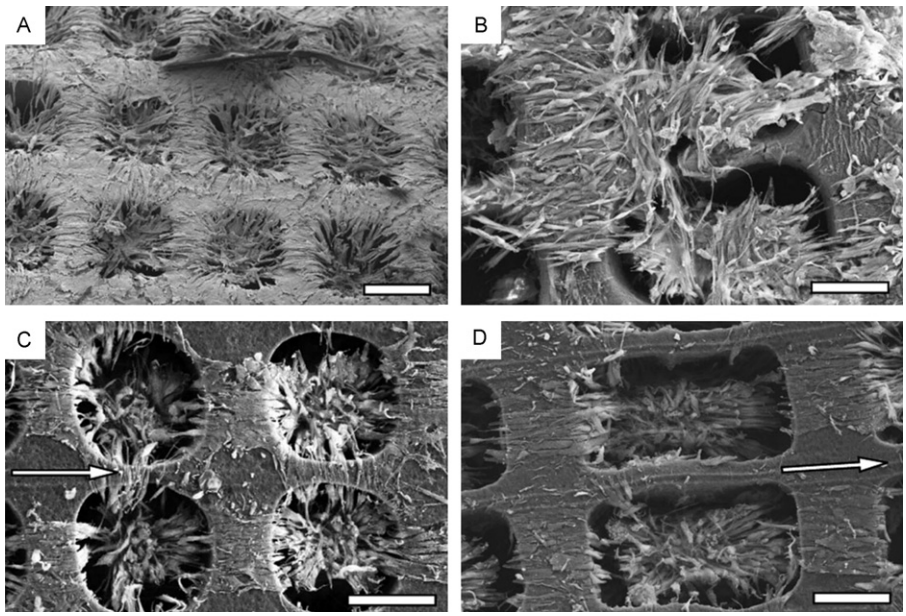

Fig. 12. Scanning electron micrographs of C2C12 muscle cells cultured on PGS scaffolds. (A and B) Square and rectangular pores without micropatterning, respectively; (C and D) square and rectangular pores with gratings, respectively. Scale bars: (A–D) 100 μm. Arrows (C and D) indicate grating direction.
From Ref. [134]. Reproduced with permission of John Wiley and Sons.

implanted subcutaneously in rats, CO scaffolds were completely integrated at 2 weeks, whereas, 13% and 16% of the NA and AL scaffolds, respectively, remained acellular. However, all scaffolds were completely populated with cells at 4 weeks post-implantation. Polarized light microscopy was used to evaluate the collagen elaboration and orientation within the scaffold. An increase in the amount of collagen was observed for CO scaffolds and enhanced alignment of the nascent collagen was observed for AL and CO scaffolds compared to NA scaffolds. These studies therefore successfully demonstrated the effect of scaffold architecture and porosity on matrix organization [146].

5.2. Designed scaffolds: 3D structures and surface topography

Scientists are increasingly looking at architectures present in nature to mimic and to overcome the structural challenges encountered during the design of scaffolds targeted for tissue engineering. One such structural arrangement is the honeycomb-like structure which is abundantly found in nature, *e.g.*, the hexagonal networks of wax built by bees, structural architecture of the native heart and the intricate trabeculations of bone. It is considered that these honeycomb like structures evolved in nature to balance mechanical properties to weight [77,154]. As discussed earlier in Section 4.1.1, Engelmayr et al. [33] fabricated accordion like PGS structures to mimic the anisotropic nature of cardiac muscles in order to maximize the functional behavior of the engineered tissue. An adaption of an accordion like structure is given in Fig. 13A.

Another interesting surface topography on acrylated PGS substrate was studied by Madhavi et al. [155]. Inspired by the nanotopography of gecko feet, which allow attachment on vertical surfaces, Madhavi et al. [155] modified the surface of PGSA films to mimic the topography of gecko feet. Gecko feet exhibits two important adhesive features of adhesion in a dry environment without a chemical glue and a fibrillar design that enhances interface compliance and conformability to surface with a variety of roughness. For the fabrication of the PGSA films nanomolds were first fabricated by using photolithography, followed by reactive ion etching of an oxide layer on a silicon wafer. The acrylated PGS prepolymer was poured into the molds and UV cured to transfer the patterned surface design from the mold to the PGSA film. Gecko patterns having different pillar size and center-to-center pitch were developed (Fig. 13B) [155].

In vitro tests have been carried out to determine the adhesiveness of nanopatterned PGSA using porcine intestinal tissue. To modulate physiological conditions, shear or sliding forces were used to mimic the potential shear forces experienced by tissue adhesives after surgical placements. *In vivo* biocompatibility studies were performed on rat models. To improve the adhesiveness, the film was also coated with oxidized dextran. These studies showed that the PGSA based adhesive invoked minimal tissue response, coating with dextran significantly increased the interfacial adhesion strength both *in vitro* and *in vivo*. The study therefore demonstrated that PGS based adhesive can have potential application for sealing wounds and for usage as sutures and staples [155]. Given the exciting results of surface designs, summarized in this section, the possibility of patterning the surface of PGS material is bound to receive further attention for advanced applications of PGS in tissue engineering.

5.3. Controlled architecture of porous PGS scaffolds to achieve vascularization

One of the main challenges faced in the engineering of artificial tissue is incorporation of stable and sustainable microvasculature in the engineered tissues. In the absence of proper vasculature engineered tissues are totally dependent on the host vasculature for oxygen, nutrients and waste removal [156–158]. Because of this dependency the thickness of the engineered tissues is limited by the mass transfer properties of the scaffold matrix. For example, without an intrinsic capillary network the maximal thickness of an engineered tissue is 150–200 μm [158–160]. Microvasculature becomes particularly important when considering tissue engineering approaches for organs such as heart, liver and kidney, which have a high metabolic demand. To address this issue of vascularization numerous biomaterial processing approaches have been reported in literature, including freeze drying, knitting, particulate leaching, selective laser sintering, stereolithography, cell-hydrogel molding and laser microablation to produce porous scaffolds, and more recently to introduce controlled capillary networks in the scaffold [54,58,161].

In this context, Fidkowski et al. [158] fabricated PGS films, into which they successfully incorporated capillary networks. To fabricate such PGS constructs, fine capillaries of 45 μm in width and 30 μm in depth were first etched onto silicon wafers by standard microelectromechanical system (MEMS) techniques. The capillary network pattern was then transferred from the silicon micromold to PGS. A flat film of PGS was also made on which inlet and outlet channels were introduced. The inlet and outlet channels in the patterned PGS film were aligned with the corresponding channels in the PGS flat film and the two layers were allowed to adhere to each other. To mimic endothelialization, the capillary networks were perfused with a syringe pump at a physiological flow rate. Following this process the device was then seeded with primary human umbilical vein endothelial cells (HUVECs). The device was endothelialized under flow conditions and part of the lumen of the capillaries reached confluence within 14 days of culture. The cells were also found to be stable under this culture conditions for at least 4 weeks [158].

Another study investigated the fabrication of three dimensional microfluidic tissue engineering vascular scaffolds based on PGS [162]. Microfluidic networks were simulated using a finite element method. Standard lithographic and plasma etching techniques were used to prepare the silicon masters for the replica molding. The PGS prepolymer was then introduced into this silicon mold and cured, thus transferring the final design to the PGS film (100 μm, thick). Devices containing up to five microfluidic layers were stacked and bonded. This was achieved easily by simply curing the polymeric films without any additional use of cytotoxic solvents or adhesives. In the final device the microchannels present had a trapezoidal

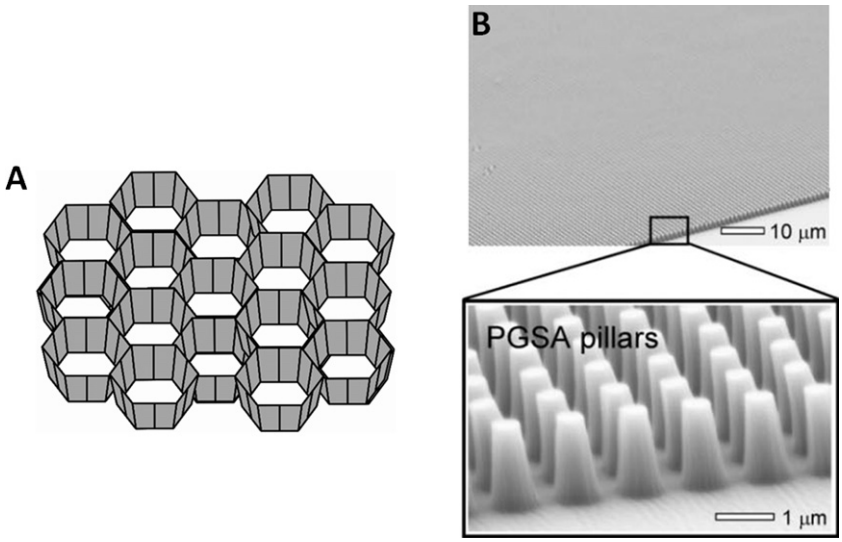

Fig. 13. Accordion like structure adapted from Engelmayr et al. [33] and (B) SEM image of incorporated gecko inspired pillar patterns on PGS matrix. From Ref. [155]. Reproduced with permission of National Academy of Sciences, United States.

shape. A successful microfluidic device must provide optimal oxygen concentration to the cells and enable exchange of nutrients and waste products. Simultaneously, the shear stresses the cells may experience within such microfluidic scaffolds may be detrimental. However, when *in vitro* cell culture studies were carried out by seeding hepatocyte carcinoma cells (HepG2), the vascular constructs exhibited constant maximum shear stress within each channel of the device [162]. This behavior mitigated the detrimental effect of shear stresses on the cells, thereby making it a promising construct for scaffolds incorporating an artificial vasculature. Fabrication of such microfluidic device using PGS also exhibited advantages over other materials used to make such devices, for example poly(dimethylsiloxane) (PDMS) and poly(lactic acid-co-glycolic acid) [162]. The major limitation of PDMS is that it is not degradable, on the other hand PLGA has been shown to be too rigid, with undesirable bulk degradation kinetics, and that high concentration of the PLGA byproducts can lead to cytotoxic effects thereby limiting its use in large organ size scaffolds [162]. Therefore, PGS with its amenable properties can be an excellent material for making such microfluidic devices aimed for various biomedical applications.

6. Modification of PGS

6.1. Composites of PGS and inorganic materials

Bioactive glasses particles have been shown to form tenacious bonds to both hard and soft tissues; bonding is enabled by the formation of a hydroxyapatite (similar to biological apatite) layer on the glass surface on exposure to biological fluids [163,164]. One such bioactive glasses attracting interest is Bioglass® 45S5 [165], which has a high bioactivity index (Class A), being osteogenetic, osteoconductive and exhibiting the ability to bond with both soft and hard connective tissues. *In vivo* work has shown that implantation of Bioglass® 45S5 in rat muscle neither calcified the muscle nor caused abnormality in organs like heart, kidney and liver [24,166–168]. By incorporating bioactive glass particles as coatings or fillers into bioresorbable polymers, composite scaffolds or structures of tailored biological and mechanical properties can be produced for applications in the engineering of various tissues [24,163,169,170]. Bioglass® 45S5 particles have also been incorporated as fillers into PGS to produce a PGS/Bioglass® composite membranes with tailorable biological and mechanical features for cardiac tissue engineering (Table 3) [24,171]. Bioglass® 45S5 porous scaffolds produced *via* a replica foam technique [172] have also been coated with PGS to produce flexible and toughened scaffolds for bone tissue engineering [173]. In any tissue engineering strategy it becomes important to tailor the rate of degradation of the scaffold to match the regenerative rate of the engineered tissue. PGS *in vivo* has been reported to undergo fast degradation, being completely absorbed within 6 weeks [3]. By incorporating Bioglass® 45S5 in PGS [24] and by coating Bioglass® scaffold with PGS [173] it was demonstrated that the degradation rate of the composite can be tailored to attenuate the material degradation kinetics to match that of the targeted tissues. This attenuation of the degradation kinetics of PGS composite by Bioglass® was in line with what has been observed with other inorganic bioceramic fillers. The combination of Bioglass® with PGS can also overcome possible problems associated with the toxicity presented by the acidic degradation products of PGS. PGS while undergoing aqueous hydrolysis of its ester groups releases carboxylic groups, which can cause localized acidic environment with pH values below physiological values. It has been reported that this localized acidity can limit the application of PGS as support material for tissue engineering applications [171]. Therefore through these studies [24,171,173] it was successfully demonstrated that PGS/Bioglass® composites overcome the problem of pH reduction owing to the PGS leachates. Addition of the inorganic fillers has also provided

Table 3
Compilation of the properties of PGS and modified PGS.[a]

PGS and its modifications	Processing parameters	E (MPa)	Ultimate tensile strength (MPa)	% elongation	T_c (°C)	T_m (°C)	Proposed applications	References
PGS	1st step: plycondensation of glycerol and sebacic acid. 2nd step: crosslinking under high vacuum and temperature	0.282–0.025	> 0.5	330%	−52.14, −18.50	5.23, 37.62	Material for soft tissue engineering	[3]
PGSA	1st step: acrylation of PGS 2nd step: crosslinking using UV rays *via* use of photoinitiator.	0.05–1.38	0.05–0.50	47.4 to 170	−32.2 (DA = 0.31) −31.1 (DA = 0.54)	–	UV crosslinked, avoids the need for crosslinking at high temperature and vacuum. Cell encapsulation	[13,180]
PSeD	Epoxide ring opening polymerization, instead of traditional polycondesation producing PGS.	1.57	1.83	409	1.2	26.4, 52.3	Proposed as second generation PGS polymer for a wide range of medical applications	[181]
PGS/Bioglass®	Bioglass® incorporated to the PGS prepolymer followed by crosslinking	0.4–1.6	0.8–1.53	180–550	–	–	Composite biomaterial for cardiac tissue engineering	[24,171]
Hybrid PGS/PCl	PGS and PCL blended at different weight ratios and electrospuned to form fibrous scaffolds *via*	8–34	1.4–2.4	400–600	–	–	Cardiovascular tissue engineering	[149]
PGSA/alginate	Fibrous scaffolds made of PGS core and alginate shell.	6.08	–	61.30	–	–	Composite biomaterial for cardiac tissue engineering	[78]

[a] DA = degree of acrylation; PCl = poly(ε-caprolactone);PGSA = acrylated PGSA; PSeD = poly(sebacoyldiglyceride); (–) = data not available.

Fig. 14. SEM image of the planar surface of the fabricated Bioglass® 45S5/PGS composite film.

additional control for tailoring the composite mechanical properties and degradation rates. Fig. 14 shows an SEM planar image of a Bioglass® 45S5/PGS fabricated in our laboratory. The composite Bioglass® 45S5/PGS films were fabricated *via* melt processing, avoiding the use of solvents such as THF and chloroform ($CHCl_3$) routinely used for such composite fabrication [24,170].

Composites of PGS and nanotubular halloysite ($2SiO_2{\cdot}2Al(OH)_2$) have also been developed for soft tissue engineering applications [174]. The nanotubular halloysite was incorporated into the PGS matrix at different wt% (1, 3, 5, 10 and 20) to produce the PGS–halloysite composites. Incorporation of the nanotubular halloysite into the PGS matrix increased the elongation to break of the composite. For example, a composite containing 20 wt% of halloysite exhibited an elongation to break of 225%, compared to a value of 110% for pure PGS. For the 1 and 5 wt% halloysite composite, mechanical properties were stable over a one-month period, making the material a candidate for mechanical support to damaged tissues during the lag phase of the healing process. Although resilience and mechanical stability improvement was observed in the PGS–halloysite composite, halloysite incorporation did not improve the problem associated with acidic pH environment caused by the degradation products of PGS [174].

6.2. Blending PGS with other polymer(s)

To date, studies on blending PGS with other polymer(s) have been mainly carried out in connection with the fabrication of electrospun fibers. Electrospinning PGS prepolymer presents difficulties because its low solution viscosity makes it difficult to spin it into fibers. This problem was overcome, for example, by blending PGS prepolymer with FDA approved biodegradable poly(ε-caprolactone) [149]. The incorporation of PCL (18–33% of total polymer blend) increased the viscosity of the blend to a level suitable for electrospinning. Blending with PCL also

offered an additional advantage as stable scaffolds could be produced without further processing, such as thermal curing or photocrosslinking. PGS and PCL were dissolved at different weight ratios (5:1, 3:1, 2:1 and 0:1, respectively) in an anhydrous chloroform:ethanol (9:1) mixture and electrospun at 12.5, 15, 17.5 and 20 kV [149]. At a given PGS:PCL ratio, higher voltages resulted in significantly smaller fiber diameters (reduced from ~4 μm to 2.8 μm). Further increase in voltage resulted in the fusion of fibers. Similarly, higher PGS concentrations in the polymer blend resulted in significantly increased fiber diameter. The mechanical properties of the PGS:PCL scaffolds were comparable to thermally or photocrosslinked polymer sheets, even though no crosslinking method was used. At the same time, PGS–PCL scaffolds did not result in decreased mechanical properties as compared to PCL-only scaffolds. Overall, the mechanical properties of the scaffolds were in the range of the native human aortic valve [175]. Interestingly, increase in the ultimate tensile strength was achieved without compromising ultimate elongation. Biological evaluation of these scaffolds showed significantly improved HUVEC attachment and proliferation compared to PCL-only scaffolds ($p < 0.05$). Thus, these study demonstrated that simple blends of PGS prepolymer with PCL can be used to fabricate microfibrous scaffolds with mechanical properties in the range of a human aortic valve leaflet [149]. In another study electrospun PGS–PCL fibers were seen to successfully support the growth and controlled differentiation of the seeded mesenchymal stem cells into vocal fold-specific, fibroblast-like cells. The MSCs, when seeded in a the micro-structured, fibrous PGS–PCL scaffold in a conditioned medium (enriched with connective tissue growth factor (CTGF) and ascorbic acid) for 21 days, expressed enhanced cell proliferation, elevated expression of fibroblast-specific protein-1, and decreased expression of mesenchymal surface epitopes without markedly triggering chondrogenesis, osteogenesis, adipogenesis, or apoptosis. At the mRNA level, CTGF supplement resulted in a decreased expression of collagen I and tissue inhibitor of metalloproteinase1, but an increased expression of decorin and hyaluronic acid synthesase 3. At the protein level, collagen I, collagen III, sulfated glycosaminoglycan, and elastin productivity was higher in the conditioned PGS–PCL culture than in the normal culture. Thus, this successful differentiation of MSCs into vocal fold-specific, fibroblast-like cells is an important step towards regeneration of damaged human vocal folds [176].

Yi and LaVan [177] fabricated PGS nanofibers by coaxial electrospinning. Various combinations were investigated, such as a mixture of PLLA and PGS prepolymer used as the core and Nylon-6 as the shell. In other versions the core was replaced by PLLA or a gelatin was mixed with PGS prepolymer to form the core shell. *In vitro* cell culture work using human dermal microvascular endothelial cells (HDMEC) showed that the cells were able to adhere and spread on the fibrous network. Cells also retained their normal phenotype thus suggesting that electrospun fibers did not have any deleterious effect on the cells [177]. Kenar et al. [178] carried out studies blending PGS with poly(3-hydroxybutyrate-co-3-hydroxyvalerate) (PHBV) and poly(L-D,L-lactic acid) (P(L-D,L)LA). The PHBV-P(L-D,L)LA-PGS (PPG) blend was electrospun into aligned fiber mats with fiber diameter ranging between 1.10 and 1.25 μm and thickness of 12 ± 3 μm. The fibrous mats were fabricated for cardiac patch application. When Human Wharton's Jelly mesenchymal stem cells were seeded into the matrix, the parallel alignment of the fibers was able to promote alignment of the seeded cells in one direction. Also the fibrous PPG mats were soft enough to be retracted by the cells. These directional alignments of the cells and softness of the mats are crucial in cardiac patch development as these would enable the seeded cardiomyocytes to have contractile activity [178].

6.3. Functionalization of PGS

One approach for improving the biocompatibility of a biomaterial is to coat its surface with relevant bioactive molecules. Coating of surfaces with cell adhesion mediators like fibronectin (FN), laminin (LM) or other ECM components enhances cell attachment, proliferation, differentiation and migration [38,179]. A similar approach was investigated to coat the surface of PGS with ECM proteins such as laminin, fibronectin, fibrin, collagen types I/III, or elastin [38]. The effect of protein coating was assessed *via in vitro* cell culture studies using peripheral blood endothelial progenitor cells. FN-precoated scaffolds stained with H&E demonstrated increased cellularity both in the luminal surface with ECM formation and "interstitial" layer of the scaffolds compared with the uncoated controls [38]. At 14 days of incubation, all precoated scaffolds demonstrated increased cellularity. Protein precoating also altered the phenotypes of endothelial progenitor cells, which resulted in changes in cellular behavior and extracellular matrix production. This study therefore suggested that using single or multiple protein precoating PGS substrates allows building and adjusting a particular biological environment to obtain cell- and tissue-specificity. In addition, the study showed that protein coated surfaces could predetermine cellular phenotypes and differentiation as well as enhance ECM formation on scaffolds [38]. In another study PGS surfaces were coated with laminin which promoted cell attachment and differentiation of retinal progenitor cells (RPC) towards mature retinal phenotype [36]. Thus scaffold precoating with bioactive proteins was shown to allow more precise engineering of cellular behavior in the development of PGS-based tissue engineering constructs [38].

7. Concluding remarks

PGS is a bioresorbable polymer produced from reactants that are intrinsic to human metabolic pathways, thus PGS is a biocompatible and bioresorbable material with increasing applications in the biomedical field, as discussed in this review. PGS presents fewer concerns in relation to immunogenic effects in comparison to natural polymers and is a flexible, elastomeric polymer that also exhibits shape memory effect. It offers additional features of tailorable mechanical properties and degradation kinetics matching those of the target tissues. Owing to these amenable features, PGS has mainly been studied for soft tissue engineering applications. Applications of

PGS have been now extended to hard tissue engineering scaffolds, control drug delivery devices and tissue adhesives. Sophisticated technologies are also being used either individually or in conjunction to generate 3D PGS porous and structured devices. These processing methods include rapid prototyping, solid-free form fabrication, micromolding, microablation and electrospinning, mainly used to fabricate structured PGS scaffolds for tissue engineering applications. Such state of the art technologies applied to PGS will play a synergistic role in providing further insight and generating knowledge on the interaction between PGS and living tissue for a variety of established and new biomedical applications of PGS.

Acknowledgment

Financial support from the EU FP-7 BIOSCENT project (ID number 214539) is acknowledged.

References

[1] Nair LS, Laurencin CT. Polymers as biomaterials for tissue engineering and controlled drug delivery. Adv Biochem Eng Biotechnol 2006;102:47–90.
[2] Bettinger CJ. Biodegradable elastomers for tissue engineering and cell–biomaterial interactions. Macromol Biosci 2011;11:467–82.
[3] Wang Y, Ameer GA, Sheppard BJ, Langer R. A tough biodegradable polymer. Nat Biotechnol 2002;20:602–6.
[4] Kemppainen JM, Hollister SJ. Tailoring the mechanical properties of 3D-designed poly(glycerol sebacate) scaffolds for cartilage applications. J Biomed Mater Res A 2010;94:9–18.
[5] Vert M, Li MS, Spenlehauer G, Guerin P. Bioresorbability and biocompatibility of aliphatic polyesters. J Mater Sci Mater Med 1992;3:432–46.
[6] Hutmacher D, Hürzeler MB, Schliephake H. A review of material properties of biodegradable and bioresorbable polymers and devices for GTR and GBR applications. Int J Oral Maxillofac Implants 1996;11:667–78.
[7] Liu G, Hinch B, Beavis AD. Mechanisms for the transport of α,ω-dicarboxylates through the mitochondrial inner membrane. J Biol Chem 1996;271:25338–44.
[8] Grego AV, Mingrone G. Dicarboxylic acids, an alternate fuel substrate in parenteral nutrition: an update. Clin Nutr 1995;14:143–8.
[9] Mortensen PB, Gregersen N. The biological origin of ketotic dicarboxylic aciduria. In vivo and in vitro investigations of the omega-oxidation of C6-C16-monocarboxylic acids in unstarved, starved and diabetic rats. Biochim Biophys Acta 1981;666:394–404.
[10] Mortensen PB. C6-C10-dicarboxylic aciduria in starved, fat-fed and diabetic rats receiving decanoic acid or medium-chain triacylglycerol. An in vivo measure of the rate of β-oxidation of fatty acids. Biochim Biophys Acta 1981;664:349–55.
[11] Tamada J, Langer R. The development of polyanhydrides for drug delivery applications. J Biomater Sci Polym Ed 1992;3:315–53.
[12] Chen QZ, Liang S, Thouas GA. Synthesis and characterisation of poly(glycerol sebacate)-co-lactic acid as surgical sealants. Soft Matter 2011;7:6484–92.
[13] Nijst CLE, Bruggeman JP, Karp JM, Ferreira L, Zumbuehl A, Bettinger CJ, Langer R. Synthesis and characterisation of photocurable elastomers from poly(glycerol-co-sebacate). Biomacromolecules 2007;8:3067–73.
[14] Ifkovits JL, Padera RF, Burdick JA. Biodegradable and radically polymerized elastomers with enhanced processing capabilities. Biomed Mater 2008;3, 034104/1–8.
[15] Dupont-Gillain CC, Nysten B, Rouxhet PG. Collagen adsorption on poly(methyl methacrylate): net-like structure formation upon drying. Polym Int 1999;48:271–6.
[16] Chen QZ, Bismarck A, Hansen U, Junaid S, Tran MQ, Harding SE, Ali NN, Boccaccini AR. Characterisation of a soft elastomer poly(glycerol sebacate) designed to match the mechanical properties of myocardial tissue. Biomaterials 2008;29:47–57.
[17] Jaafer IH, Ammar MM, Jedlicka SS, Pearson RA, Coulter JP. Spectroscopic evaluation, thermal, and thermomechanical characterization of poly(glycerol-sebacate) with variations in curing temperatures and durations. J Mater Sci 2010;45:2525–9.
[18] Manzanedo D. Biorubber (PGS): evaluation of a novel biodegradable elastomer. MEng thesis. Boston: Department of Materials Science and Engineering, Massachusetts Institute of Technology; 2006. 51 pp.
[19] Sundback CA, Shyu JY, Wang Y, Faquin WC, Langer RS, Vacanti JP, Hadlock TA. Biocompatibility analysis of poly-(glycerol sebacate) as a nerve guide material. Biomaterials 2005;26:5454–64.
[20] Yamaguchi S. Analysis of stress–strain curves at fast and slow velocities of loading in vitro in the transverse section of the rat incisor periodontal ligament following the administration of aminopropionitrile. Arch Oral Biol 1992;37:439–44.
[21] Komatsu K, Chiba M. The effect of velocity of loading on the biomechanical responses of the periodontal ligament in transverse sections of the rat molar *in vitro*. Arch Oral Biol 1993;38:369–75.
[22] Lee MC, Haut RC. Strain rate effects on tensile failure properties of the common carotid artery and jugular veins of ferrets. J Biomech 1992;25:925–7.
[23] Liu Q, Tian M, Shi R, Zhang L, Chen D, Tian W. Structure and properties of thermoplastic poly(glycerol sebacate) elastomers originating from prepolymers with different molecular weights. J Appl Polym Sci 2007;104:1131–7.
[24] Liang SL, Cook WD, Thouas GA, Chen QZ. The mechanical characteristics and in vitro biocompatibility of poly(glycerol sebacate)—bioglass elastomeric composites. Biomaterials 2010;31:8516–29.
[25] Cai W, Liu C. Shape-memory effect of poly (glycerol-sebacate) elastomer. Mater Lett 2008;62:2171–3.
[26] Preusting H, Nijenhuis A, Witholt B. Physical characteristics of poly(3-hydroxyalkanoates) and poly(3-hydroxyalkenoates) produced by *Pseudomonas oleovorans* grown on aliphatic hydrocarbons. Macromolecules 1990;23:4220–4.
[27] Sánchez R, Schripsema J, da Silva LF, Taciro MK, Pradella GC, Gomez GC. Medium-chain-length polyhydroxyalkanoic acids (PHAmcl) produced by *Pseudomonas putida* IPT 046 from renewable sources. Eur Polym J 2003;39:1385–94.
[28] Chen QZ, Ishii H, Thouas GA, Lyon AR, Wright JS, Blaker JJ, Chirzanowski W, Boccaccini AR, Ali NN, Knowles JC, Harding SE. An elastomeric patch derived from poly(glycerol sebacate) for delivery of embryonic stem cells to the heart. Biomaterials 2010;31:3885–93.
[29] Wang Y, Kim YM, Langer R. *In vivo* degradation characteristics of poly(glycerol sebacate). J Biomed Mater Res A 2003;66:192–7.
[30] Liang SL, Yang XY, Fang XY, Cook WD, Thouas GA, Chen QZ. In vitro enzymatic degradation of poly (glycerol sebacate)-based materials. Biomaterials 2011;32:8486–96.
[31] Sun ZJ, Wu L, Huang W, Chen C, Chen Y, Lu X, Zhang XL, Yang BF, Dong DL. Glycolic acid modulates the mechanical property and degradation of poly(glycerol, sebacate, glycolic acid). J Biomed Mater Res A 2010;92:332–9.
[32] Wang YX, Robertson Jr JL, Spillman WB, Claus RO. Effects of the chemical structure and the surface properties of polymeric biomaterials on their biocompatibility. Pharmaceut Res 2004;21:1362–73.
[33] Engelmayr GC, Cheng M, Bettinger CJ, Borenstein JT, Langer R, Freed LE. Accordion-like honeycombs for tissue engineering of cardiac anistropy. Nat Mater 2008;7:1003–10.
[34] Crapo PM, Wang Y. Pysiologic compliance in engineered small diameter arterial constructs based on an elastomeric substrate. Biomaterials 2010;31:1626–35.
[35] Gao J, Ensley AE, Nerem RM, Wang Y. Poly(glycerol sebacate) supports the proliferation and phenotypic protein expression of primary baboon vascualr cells. J Biomed Mater Res A 2007;83:1070–5.
[36] Redenti S, Neeley WL, Rompani S, Saigal S, Yang J, Klassen H, Langer R, Young MJ. Engineering retinal progenitor cell and scrollable poly(glycerol-sebacate) composites for expansion and subretinal transplantation. Biomaterials 2009;30:3405–14.
[37] Rai R, Keshavarz T, Roether JA, Boccaccini AR, Roy I. Medium chain length polyhydroxyalkanoates, promising new biomedical materials for the future. Mat Sci Eng R 2010;72:29–47.
[38] Sales VL, Engelmayr Jr GC, Johnson JA, Wang Y, Sacks MS, Mayer Jr JE. Protein precoating of elastomeric tissue-engineering scaffolds increased cellularity. Enhanced extracellular matrix protein production, and differentially regulated the phenotypes of circulating endothelial progenitor cells. Circulation 2007;116:55–63.

[39] Hurrell S, Milroy GE, Cameron RE. The degradation of polyglycolide in water and deuterium oxide. Part I: the effect of reaction rate. Polymer 2003;44:1421–4.
[40] Böstman OM, Laitinen OM, Tynninen O, Salminen ST, Pihlajamäki HK. Tissue restoration after resorption of polyglycolide and poly-laevo-lactic acid screws. J Bone Joint Surg Br 2005;87B: 1575–80.
[41] Subramanian A, Krishnan UM, Sethuraman S. Fabrication of uniaxially aligned 3D electrospun scaffolds for neural regeneration. Biomed Mater 2011;6, 025004/1–10.
[42] Damadzadeh B, Jabari H, Skrifvars M, Airola K, Moritz N, Vallittu PK. Effect of ceramic filler content on the mechanical and thermal behavior of poly-L-lactic acid and poly-L-lactic-co-glycolic acid composites for medical applications. Mater Sci Mater Med 2010;21:2523–31.
[43] Zhang D, Kandadai MA, Cech J, Roth S, Curran SA. Poly(L-lactide) (PLLA)/multi-walled carbon nanotube (MWCNT) composite: characterisation and biocompatibility evaluation. J Phys Chem B 2006;110:12910–5.
[44] Radford MJ, Noakes J, Read J, Wood DG. The natural history of a bioabsorbable interference screw used for anterior cruciate ligament reconstruction with a 4-strand hamstring technique. Arthroscopy 2005;21:707–10.
[45] Walton M, Cotton NJ. Long-term in vivo degradation of poly-L-lactide (PLLA) in bone. J Biomater Appl 2007;21:395–411.
[46] Eshraghi S, Das S. Mechanical and microstructural properties of polycaprolactone scaffolds with one-dimensional, two-dimensional, and three-dimensional orthogonally oriented porous architectures produced by selective laser sintering. Acta Biomater 2010;6:2467–76.
[47] Lam CXF, Hutmacher DW, Schantz JT, Woodruff MA, Teoh SH. Evaluation of polycaprolactone scaffold degradation for 6 months *in vitro* and *in vivo*. J Biomed Mater Res A 2008;90:906–19.
[48] Lam CXF, Salvani MM, Teoh SH, Hutmacher DW. Dynamics of in vitro polymer degradation of polycaprolactone-based scaffolds: accelerated versus simulated physiological conditions. Biomed Mater 2008;3, 03410/1–15.
[49] Taguchi K, Taguchi S, Sudesh K, Maehara A, Takeharu T, Doi Y. Metabolic pathways and engineering of PHA biosynthesis. In: Doi Y, Steinbuchel A, editors. Biopolymers: polyesters. Wiley-VCH: Weinheim; 2002. p. 217–372.
[50] Williams SF, Martin DP. Applications of PHAs in medicine and pharmacy. In: Steinbüchel A, Marchessault RH, editors. Biopolymers for medicinal and pharmaceutical applications. Wiley-VCH: Weinheim; 2005. p. 91–127.
[51] Williams SF, Martin DP, Horowitz DM, Peoples OP. PHA applications: addressing the price performance issue. I. Tissue engineering. Int J Biol Macromol 1999;25:111–21.
[52] Lanza R, Langer R, vacant R, editors. Principles of tissue engineering. San Diego, CA: Elsevier Academic Press; 2007.
[53] Anon. World Health Organization factsheet on cardiovascular disease. http://www.who.int/mediacentre/factsheets/fs317/en/index.html [web address accessed on January 2011; 2011 fact sheet no. 317].
[54] Chiu LLY, Radisic M, Novakovic GV. Bioactive scaffolds for engineering vascularised cardiac tissues. Macromol Biosci 2010;10:1286–301.
[55] Sun Y, Weber KT. Infarct scar: a dynamic tissue. Cardiovasc Res 2000;46:250–6.
[56] Christman KL, Lee RJ. Biomaterials for the treatment of myocardial infarction. J Am Coll Cardiol 2006;5:907–13.
[57] Mann DL. Mechanisms and models in heart failure: a combinatorial approach. Circulation 1999;100:999–1008.
[58] Radisic M, Novakovic GV. Cardiac tissue engineering. J Serb Chem Soc 2005;70:541–56.
[59] Leor J, Amsalem Y, Cohen S. Cells, scaffolds and molecules for mycardial tissue engineering. Pharmacol Ther 2005;105:151–63.
[60] Jean A, Engelmayr Jr GC. Finite element analysis of an accordion-like honeycomb scaffold for cardiac tissue engineering. J Biomech 2010;43:3035–43.
[61] Radisc M, Park H, Martens TP, Lazaro JES, Geng W, Wang Y, Langer R, Freed LE, Novakovic GV. Pre-treatment of synthetic elastomeric scaffold by cardiac fibroblast improves engineered heart tissue. J Biomed Mater Res A 2008;86:713–24.
[62] Radisic M, Deen W, Langer R, Vunjak-Novakovic G. Mathematical model of oxygen distribution in engineered cardiac tissue with parallel channel array perfused with culture medium containing oxygen carriers. Am J Physiol Heart Circ Physiol 2005;288:H1278–89.
[63] Radisic M, Marsano A, Maidhof R, Wang Y, Novakovic GV. Cardiac tissue engineering using perfusion bioreactor systems. Nat Protoc 2008;3:719–38.
[64] Radisic M, Park H, Chen F, Lazzaro JES, Wang Y, Denns R, Langer R, Freed L, Novakovic GV. Biomimetic approach to cardiac tissue engineering: oxygen carriers and channeled scaffolds. Tissue Eng 2006;12:2077–91.
[65] Park H, Larson BL, Guillemette MD, Jain SR, Hua C, Engelmayr Jr GC, Freed L. The significance of pore microarchitecture in a multi-layered elastomeric scaffold for contractile cardiac muscle constructs. Biomaterials 2011;32:1856–64.
[66] Bhana B, Iyer RK, Chen WLK, Zhao R, Sider KL, Likhitpanichkul M, Simmons CA, Radisc M. Influence of substrate stiffness on the phenotype of heart cells. Biotechnol Bioeng 2010;105:1148–60.
[67] Gaudesius G, Miragoli M, Thomas SP, Rohr S. Coupling of cardiac electrical activity over extended distances by fibroblasts of cardiac origin. Circ Res 2003;93:421–8.
[68] Sussman MA, McCulloch A, Borg TK. Dance band on the titanic: biomechanical signaling in cardiac hypertrophy. Circ Res 2002;91:888–98.
[69] Rudy Y. Conductive bridges in cardiac tissue: a beneficial role or an arrhythmogenic substrate? Circ Res 2004;94:709–11.
[70] Camelliti P, Borg TK, Kohl P. Structural and functional characterisation of cardiac fibroblasts. Cardiovasc Res 2005;65:40–51.
[71] Kohl P. Heterogeneous cell coupling in the heart: an electrophysiological role for fibroblasts. Circ Res 2003;93:381–3.
[72] Porter KE, Turner NA. Cardiac fibroblast: at the heart of myocardial remodeling. Pharmacol Ther 2009;123:255–78.
[73] Zimmermann WH. Tissue engineering: polymer flex their muscles. Nat Mater 2008;7:932–3.
[74] Dvir T, Levy O, Shachar M, Granot Y, Cohen S. Activation of the ERK1/2 cascade via pulsatile interstitial fluid flow promotes cardiac tissue assembly. Tissue Eng 2007;13:2185–93.
[75] Macchiarelli G, Ohtani O, Nottola SA, Stallone T, Camboni A, Prado IM, Motta PM. A micro-anatomical model of the distribution of myocardial endomysial collagen. Histol Histopathol 2002;17:699–706.
[76] Pope AJ, Sands GB, Smaill BH, LeGrice IJ. Three-dimensional transmural organization of perimysial collagen in the heart. Am J Physiol Heart Circ Physiol 2008;295:H1243–52.
[77] Freed LE, Engelmayr GCJ, Borenstein JT, Moutos FT, Guilak F. Advanced material strategies for tissue engineering scaffolds. Adv Mater 2009;21:3410–8.
[78] Ravichandran R, Venugopal JR, Sundarrajan S, Mukherjee S, Ramakrishna S. Poly(glycerol sebacate)/gelatin core/shell fibrous structure for regeneration of myocardial infarction. Tissue Eng Part A 2011;17:1363–73.
[79] Stuckey DJ, Ishii H, Chen QZ, Boccaccini AR, Hansen U, Carr CA, Roether JA, Jawad H, Tyler DJ, Ali NN, Clarke K, Harding SE. Magnetic resonance imaging evaluation of remodeling by cardiac elastomeric tissue scaffold biomaterials in a rat model of myocardial infarction. Tissue Eng Part B 2010;16:3395–402.
[80] Gao J, Crapo PM, Wang YD. Macroporous elastomeric scaffolds with extensive micropores for soft tissue engineering. Tissue Eng 2006;12:917–25.
[81] Crapo PM, Gao J, Wang H. Seamless tubular poly(glycerol sebacate) scaffolds: high yield and fabrication and potential applications. J Biomed Mater Res A 2007;86:354–63.
[82] Lee KW, Stolz DB, Wang Y. Substantial expression of mature elastin in arterial constructs. Proc Natl Acad Sci USA 2010;108:2705–10.
[83] Motlagh D, Yang J, Lui KY, Webb AR, Ameer GA. Hemocompatibility evaluation of poly(glycerol-sebacate) in vitro for vascular tissue engineering. Biomaterials 2006;27:4315–24.
[84] D'Armiento J. Decreased elastin in vessel walls puts the pressure on. J Clin Invest 2003;112:1308–10.
[85] Qu XH, Wu Q, Chen GQ. *In vitro* study on hemocompatibility and cytocompatibility of poly(3-hydroxybutyrate-co-3-hydroxyhexanoate). J Biomater Sci Polym Ed 2006;17: 1107–21.
[86] Mow VC, Guo XE. Mechano-electromechanical properties of articular cartilage: their inhomogeneities and anisotropies. Annu Rev Biomed Eng 2002;4:175–209.
[87] Jeong CG, Hollister SJ. A comparison of the influence of material on in vitro cartilage tissue engineering with PCL, PGS, and POC 3D scaffold architecture seeded with chondrocytes. Biomaterials 2010;31:4304–12.
[88] Pritchard CD, Arnér KM, Langer RS, Ghosh FK. Retinal transplantation using surface modified poly(glycerol-co-sebacic acid) membranes. Biomaterials 2010;31:7978–84.

[89] Pritchard CD, Arnér KM, Neal RA, Neeley WL, Bojo P, Bachelder E, Holz J, Watson N, Botchwey EA, Langer RS, Ghosh FK. The use of surface modified poly(glycerol-co-sebacic acid) in retinal transplantation. Biomaterials 2010;31:2153–62.
[90] Neeley WL, Redenti S, Klassen H, Tao S, Desai T, Young MJ, Langer R. A microfabricated scaffold for retinal progenitor cell grafting. Biomaterials 2008;29:418–26.
[91] Ghosh FK, Neeley WL, Arnér KM, Langer R. Selective removal of photoreceptor cells in vivo using the biodegradable elastomer poly(glycerol sebacate). Tissue Eng Part A 2009;17:1675–82.
[92] Hynes SR, Lavik EB. A tissue-engineered approach towards retinal repair: scaffolds for cell transplantation to the subretinal space. Graefes Arch Clin Exp Ophthalmol 2010;248:763–78.
[93] Lundborg G. Nerve injury and repair. New York: Longman Group UK Ltd; 1988.
[94] Widmer MS, Gupta PK, Lu L, Meszlenyi RK, Evans GR, Brandt K, Savel T. Manufacture of porous biodegradable polymer conduits by an extrusion process for guided tissue regeneration. Biomaterials 1998;19:1945–55.
[95] Evans GR, Brandt K, Widmer MS, Lu L, Meszlenyi RK, Gupta PK, Mikos AG. In vivo evaluation of poly(L-lactic acid) porous conduits for peripheral nerve regeneration. Biomaterials 1999;20:1109–15.
[96] Hadlock T, Sundback C, Hunter D, Cheney M, Vacanti JP. A polymer foam conduit seeded with Schwann cells promotes guided peripheral nerve regeneration. Tissue Eng Part B 2006;6:119–27.
[97] den Dunnen WF, van der Lei B, Schakenraad JM, Stokroos I, Blaauw E, Bartels H, Pennings AJ. Poly(DL-lactide-epsiloncaprolactone) nerve guides perform better than autologous nerve grafts. Microsurgery 1996;17:348–57.
[98] Rodriguez FJ, Gomez N, Perego G, Navarro X. Highly permeable polylactide-caprolactone nerve guides enhance peripheral nerve regeneration through long gaps. Biomaterials 1999;20:1489–500.
[99] Valero-Cabre A, Tsironis K, Skouras E, Perego G, Navarro X, Neiss WF. Superior muscle reinnervation after autologous nerve graft or poly-L-lactide-epsilon-caprolactone (PLC) tube implantation in comparison to silicone tube repair. J Neurosci Res 2001;63:214–23.
[100] Robinson PH, van der LB, Hoppen HJ, Leenslag JW, Pennings AJ, Nieuwenhuis P. Nerve regeneration through a two-ply biodegradable nerve guide in the rat and the influence of ACTH4-9 nerve growth factor. Microsurgery 1991;12:412–9.
[101] Langone F, Lora S, Veronese FM, Caliceti P, Parnigotto PP, Valenti F, Palma G. Peripheral nerve repair using a poly(organo) phosphazene tubular prosthesis. Biomaterials 1995;16:347–53.
[102] Schappacher M, Fabre T, Mingotaud AF, Soum A. Study of a (trimethylenecarbonate-co-epsilon-caprolactone) polymer. Part 1: preparation of a new nerve guide through controlled random copolymerization using rare earth catalysts. Biomaterials 2001;22:2849–55.
[103] Fabre T, Schappacher M, Bareille R, Dupuy B, Soum A, Bertrand-Barat J, Baquey C. Study of a (trimethylenecarbonate-co-epsilon-caprolactone) polymer. Part 2: in vitro cytocompatibility analysis and in vivo ED1 cell response of a new nerve guide. Biomaterials 2001;22:2951–8.
[104] Pego AP, Poot AA, Grijpma DW, Feijen JJ. Copolymers of trimethylene carbonate and epsilon-caprolactone for porous nerve guides: synthesis and properties. Biomater Sci Polym Ed 2001;12:35–53.
[105] Rydevik BL, Kwan MK, Myers RR, Brown RA, Triggs KJ, Woo SL, Garfin SR. An in vitro mechanical and histological study of acute stretching on rabbit tibial nerve. J Orthop Res 1990;8:694–701.
[106] den Dunnen WF, van der L, Robinson B, Holwerda PH, Pennings A, Schakenraad AJJM. Biological performance of a degradable poly(lactic acid-epsilon-caprolactone) nerve guide: influence of tube dimensions. J Biomed Mater Res A 1995;29:757–66.
[107] Henry EW, Chiu TH, Nyilas E, Brushart TM, Dikkes P, Sidman RL. Nerve regeneration through biodegradable polyester tubes. Exp Neurol 1985;90:652–76.
[108] Anon. Vital and health statistics report. Ambulatory and inpatient procedures in the United States. Washington, DC: US Department of Health and Human Services; US Government Printing Office; 1996.
[109] Wieland AM, Sundback C, Hart A, Kulig K, Masiakos PT, Hartnick CJ. Poly(glycerol sebacate)-engineered plugs to repair chronic tympanic membrane perforations in a chinchilla model. Otolaryngol Head Neck Surg 2010;143:127–33.
[110] Fayad JN, Baino T, Parisier SC. Preliminary results with the use of AlloDerm in chronic otitis media. Laryngoscope 2003;113:1228–30.
[111] Laidlaw DW, Costantino PD, Govindaraj S, Hiltzik DH, Catalano PJ. Tympanic membrane repair with a dermal allograft. Laryngscope 2001;111:702–7.
[112] Ladewiq K. Drug delivery in soft tissue engineering. Expert Opin Drug Deliv 2011;8:1175–88.
[113] Papkov MS, Agashi K, Olaye A, Shakesheff K, Domb AJ. Polymer carriers for drug delivery in tissue engineering. Adv Drug Delivery Rev 2001;59:187–206.
[114] Mourino V, Boccaccini AR. Bone tissue engineering therapeutics: controlled drug delivery in three-dimensional scaffolds. J R Soc Interface 2010;7:209–27.
[115] Sun ZJ, Chen C, Sun MZ, Hong C, Lu XL, Zheng YF, Yang BF, Dong DL. The application of poly (glycerol-sebacate) as biodegradable drug carrier. Biomaterials 2009;30:5209–14.
[116] Tobias IS, lee H, Engelmayr Jr GC, Macaya D, Bettinger CJ, Cima MJ. Zero-order controlled release of ciprofloxacin-HCl from a reservoir-based, bioresorbable and elastomeric device. J Control Release 2010;146:356–62.
[117] Becker JM, Stucchi AF. Intra-abdominal adhesion prevention: are we getting any closer? Ann Surg 2004;240:202–4.
[118] Menzies D, Ellis H. Intestinal obstruction from adhesions—how big is the problem? Ann R Coll Surg Engl 1990;72:60–3.
[119] Pryor HI, O'Doherty E, Hart A, Owens G, Hoganson D, Vacanti JP, Masiakos T, Sundback CA. Poly(glycerol sebacate) films prevent postoperative adhesions and allow laparoscopic placement. Surgery 2009;146:490–7.
[120] Menzies D. Postoperative adhesions: their treatment and relevance in clinical practice. Ann R Coll Surg Engl 1993;75:147–53.
[121] Holmdahl L. Making and covering of surgical footprints. Lancet 1999;353:1456–7.
[122] Attard JA, MacLean AR. Adhesive small bowel obstruction: epidemiology, biology and prevention. Can J Surg 2007;50:291–300.
[123] Avital S, Bollinger TJ, Wilkinson JD, Marchetti F, Hellinger MD, Sands LR. Preventing intra-abdominal adhesions with polylactic acid film: an animal study. Dis Colon Rectum 2005;48:153–7.
[124] Burns JW, Colt MJ, Burgees LS, Skinner KC. Preclinical evaluation of seprafilm bioresorbable membrane. Eur J Surg Suppl 1997;(577):40–8.
[125] Zong X, Li S, Chen E, Garlick B, Kim KS, Fang D. Prevention of postsurgery-induced abdominal adhesions by electrospun bioabsorbable nanofibrous poly(lactide-co-glycolide)-based membranes. Ann Surg 2004;240:910–5.
[126] De Cherney AH, di Zerega GS. Clinical problem of intraperitoneal postsurgical adhesion formation following general surgery and the use of adhesion prevention barriers. Surg Clin North Am 1997;77:671–88.
[127] Becker JM, Dayton MT, Fazio VW, Beck DE, Stryker SJ, Wexner SD. Prevention of postoperative abdominal adhesions by a sodium hyaluronate-based bioresorbable membrane: a prospective, randomized, double-blind multicenter study. J Am Coll Surg 1996;183:297–306.
[128] Cohen Z, Senagore AJ, Dayton MT, Koruda MJ, Beck DE, Wolff BG. Prevention of postoperative abdominal adhesions by a novel, glycerol/sodium hyaluronate/carboxymethylcellulose-based bioresorbable membrane: a prospective, randomized, evaluator-blinded multicenter study. Dis Colon Rectum 2005;48:1130–9.
[129] Takeuchi H, Kitade M, Kikuchi I, Shimanuki H, Kinoshita K. A novel instrument and technique for using seprafilmhyaluronic acid/carboxymethylcellulose membrane during laparoscopic myomectomy. J Laparoendosc Adv Surg Tech A 2006;16:497–502.
[130] Philip S, Keshavarz T, Roy I, Polyhydroxyalkanoates:. biodegradable polymers with a range of applications. J Chem Technol Biotechnol 2007;82:233–47.
[131] Bettinger CJ, Orrick B, Misra A, Langer R, Borenstein JT. Microfabrication of poly (glycerol-sebacate) for contact guidance applications. Biomaterials 2006;27:2558–65.
[132] Timpl R. Macromolecular organization of basement membranes. Curr Opin Cell Biol 1996;8:618–24.
[133] Abrams GA, Schaus SS, Goodman SL, Nealey PF, Murphy CJ. Nanoscale topography of the corneal epithelial basement membrane and Descemet's membrane of the human. Cornea 2000;19:57–64.
[134] Guillemette MD, Park H, Hsiao JC, Jain SR, Larson BL, Langer R, Freed LE. Combined technologies for microfabricating elastomeric cardiac tissue engineering scaffolds. Macromol Biosci 2010;10:1330–7.
[135] Teixeira AI, Abrams GA, Bertics PJ, Murphy CJ, Nealey PF. Epithelial contact guidance on well-defined micro- and nanostructured substrates. J Cell Sci 2003;116:1881–92.
[136] Karuri NW, Liliensiek S, Teixeira AI, Abrams G, Campbell S, Nealey PF. Biological length scale topography enhances cell

substratum adhesion of human corneal epithelial cells. J Cell Sci 2004;117:3153–64.
[137] Brunette DM. Spreading and orientation of epithelial cells on grooved substrata. Exp Cell Res 1986;167:203–17.
[138] Walboomers XF, Croes H, Gensel LA, Jansen JA. Contact guidance of rat fibroblasts on various implant materials. J Biomed Mater Res 1999;47:204–12.
[139] Walboomers XF, Monaghan W, Curtis A, Jansen JA. Attachment of fibroblasts on smooth and microgrooved polystyrene. J Biomed Mater Res 1999;46:212–20.
[140] Braber ET, Ruijter JE, Smits H, Ginsel LA, Recum AF, Jansen JA. Quantitative analysis of fibroblast morphology on microgrooved surfaces with various groove and ridge dimensions. Biomaterials 1996;17:2037–44.
[141] Webb A, Clark P, Skepper J, Compston A, Wood A. Guidance of oligodendrocytes and their progenitors by substratum topography. J Cell Sci 1995;108:2747–60.
[142] Ramakrishna S, Fujihara K, Teo WE, Lim TC, Ma P. An introduction to electrospinning and nanofibers. Singapore: World Scientific Publishing Co Pte Ltd; 2005.
[143] Sell SA, Wolfe PS, Garg K, McCool JM, Rodriguez IA, Bowlin GL. The use of natural polymers in tissue engineering: a focus on electrospun extracellular matrix analogues. Polymers 2010;2:522–53.
[144] Baker BM, Handorf AM, Ionescu LC, Li WJ, Mauck RL. New directions in nanofibrous scaffolds for soft tissue engineering and regeneration. Expert Rev Med Dev 2009;6:515–32.
[145] Rockwood DN, Akins RE, Parrag IC, Woodhouse KA, Rabolt JF. Culture on electrospun polyurethane scaffolds decreases atrial natriuretic peptide expression by cardiomyocytes in vitro. Biomaterials 2008;29:4783–91.
[146] Ifkovits JL, Wu K, Mauck RL, Burdick JA. The influence of fibrous elastomer structure and porosity on matrix organization. PLoS ONE 2010;5(12), e15717/1–10.
[147] Li CM, Vepari C, Jin HJ. Electrospun silk-BMP-2 scaffolds for bone tissue engineering. Biomaterials 2006;27:3115–24.
[148] Liao S, Li B, Ma Z. Biomimetic electrospun nanofibers for tissue regeneration. Biomed Mater 2006;1:45–53.
[149] Sant S, Hwang CM, Lee SH, Khademhosseini A. Hybrid PGS–PCL microfibrous scaffolds with improved mechanical and biological properties. J Tissue Eng Regen Med 2010;5:283–91.
[150] Mauck RL, Baker BM, Nerurkar NL. Engineering on the straight and narrow: the mechanics of nanofibrous assemblies for fiber-reinforced tissue regeneration. Tissue Eng Part B 2009;15:171–93.
[151] Sacks MS, Schoen FJ, Mayer JE. Bioengineering challenges for heart valve tissue engineering. Annu Rev Biomed Eng 2009;11:289–313.
[152] Khademhosseini A, Langer R, Borenstein J, Vacanti JP. Microscale technologies for tissue engineering and biology. Proc Natl Acad Sci USA 2006;103:2480–7.
[153] Hwang CM, Park Y, Park JY. Controlled cellular orientation on PLGA microfibers with defined diameters. Biomed Microdevices 2009;11:739–46.
[154] Gibson LJ. Biomechanics of cellular solids. J Biomech 2005;38:377–99.
[155] Madhavi A, Ferreira L, Sundback C, Nichol JW, Chan EP, Carter DJD, Bettinger CJ, Patanavanich S, Chignozha L, Joseph EB, Galakatos A, Pryror H, Pomerantseva I, Masiakos PT, Faquin W, Zumbuehl A, Hong S, Borenstein J, Vacanti J, Langer R, Karp JM. A biodegradable and biocompatible gecko-inspired tissue adhesive. Proc Natl Acad Sci USA 2008;105:2307–12.
[156] Vacanti JP, Langer R. Tissue engineering: the design and fabrication of living replacement devices for surgical reconstruction and transplantation. Lancet 1999;354:532–4.
[157] Langer R, Vacanti JP. Tissue engineering: the challenges ahead. Sci Am 1999;280:86–9.
[158] Fidowski C, Mofrad MRK, Borenstein J, Vacanti JP, Langer R, Wang YW. Endothelialized microvasculature based on a biodegradable elastomer. Tissue Eng 2005;11:302–9.
[159] Colton CK. Implantable biohybrid artificial organs. Cell Transplant 1995;4:414–36.
[160] Folkman J, Hochberg M. Self-regulation of growth in three dimensions. J Exp Med 1973;138:745–53.
[161] Novakovic GV, Tandon N, Godier A, Maidhof R, Marsano A, Martens TP, Radisc M. Challenges in cardiac tissue engineering. Tissue Eng Part B 2010;16:169–87.
[162] Bettinger CJ, Weinberg EJ, Kulig KM, Vacanti JP, Wang Y, Borenstein JT, Langer R. Three dimensional microfluidic tissue engineering scaffolds using a flexible biodegradable polymer. Adv Mater 2005;18:165–9.
[163] Misra SK, Valappil SP, Roy I, Boccaccini AR. Polyhydroxyalkanoate (PHA)/inorganic phase composites for tissue engineering applications. Biomacromolecules 2006;7:2249–58.
[164] Roether JA, Boccaccini AR, Hench LL, Maquet V, Gautier S, Jérôme R. Development and in-vitro characterisation of novel bioresorbable and bioactive composite materials based on polylactide foams and Bioglass (R) for tissue engineering applications. Biomaterials 2002;23:3871–8.
[165] Hench LL, Bioceramics. J Am Ceram Soc 1998;81:1705–28.
[166] Merolli A, Leali PT, Guidi PL, Gabbi C. Comparison in in vivo response between a bioactive glass and a non-bioactive glass. J Mater Sci: Mater Med 2000;11:219–22.
[167] Lai W, Garino J, Flaitz C, Ducheyne P. Excretion of resorption products from bioactive glass implanted in rabbit muscle. J Biomed Mater Res A 2005;75:398–407.
[168] Lai W, Ducheyne P, Garino J, Flaitz CM. Removal pathway of bioactive glass resorption products from the body. Mater Res Soc Symp Proc 2000;599:261–6.
[169] Misra SK, Nazhat SN, Valappil SP, Torbati MM, Wood RJK, Roy I, Boccaccini AR. Fabrication and characterization of biodegradable poly(3-hydroxybutyrate) composite containing bioglass. Biomacromolecules 2007;8:2112–9.
[170] Rai R, Boccaccini AR, Knowles JC, Locke IC, Gordgee MP, McCormick A, Salihd V, Mordon N, Keshavarz T, Roy I. Fabrication of a novel poly(3-hydroxyoctanoate)/nanoscale bioactive glass composite film with potential as a multifunctional wound dressing. AIP Conf Proc 2010;1255:126–8.
[171] Chen Q, Jin L, Cook WD, Mohn D, Lagerqvist EL, Elliott DA, Haynes JM, Boy N, Stark WJ, Pouton CW, Stanley EG, Elefanty AG. Elastomeric nanocomposites as cell delivery vehicles and cardiac support devices. Soft Matter 2010;6:4715–26.
[172] Chen QZ, Thompson ID, Boccaccini AR. 45S5 Bioglass®-derived glass-ceramic scaffolds for bone tissue engineering. Biomaterials 2006;27:2414–25.
[173] Chen QZ, Quinn JMW, Thouas GA, Zhou X, Komesaroff PA. Bone-like elastomeric toughened scaffolds with degradability kinetics matching healing rates. Adv Eng Mater 2010;12:B642–8.
[174] Chen QZ, Liang SL, Wang J, Simon GP. Manipulation of mechanical compliance of elastomeric PGS by incorporation of halloysite nanotubes for soft tissue engineering applications. J Mech Behav Biomed Mater 2011;4:1805–18.
[175] Balguid A, Rubbens MP, Mol A, Bank RA, Bogers AJ, van Kats JP, de Mol BA, Baaijens FP, Bouten CV. The role of collagen cross-links in biomechanical behavior of human aortic heart valve leaflets – relevance for tissue engineering. Tissue Eng 2007;13:1501–11.
[176] Tong Z, Sant S, Khademhosseini A, Ji X. Controlling the fibroblastic differentiation of mesenchymal stem cells via the combination of fibrous scaffolds and connective tissue growth factor. Tissue Eng Part A 2011;21:2773–85.
[177] Yi F, LaVan DA. Poly(glycerol sebacate) nanofiber scaffolds by core/shell electrospinning. Macromol Biosci 2008;8:803–6.
[178] Kenar H, Kose GT, Hasirci V. Design of a 3D aligned myocardial tissue construct from biodegradable polyesters. J Mater Sci Med 2010;21:989–97.
[179] Balcells M, Edelman ER. Effect of pre-adsorbed proteins on attachment, proliferation, and function of endothelial cells. J Cell Physiol 2002;191:155–61.
[180] Gerechta S, Townsend SA, Presslerc H, Zhu H, Nijst CLE, Bruggemang JP, Nichola JW, Langer R. A porous photocurable elastomer for cell encapsulation and culture. Biomaterials 2007;28:4826–35.
[181] You Z, Cao H, Gao J, Shin PH, Day BW, Wang Y. A functionalized polyester with free hydroxyl groups and tunable physiochemical and biological properties. Biomaterials 2010;31:3129–38.